
Modelling as a tool to augment ground motion data in regions of diffuse seismicity -
Progress 2015

Ludovic Fülöp¹, Vilho Jussila¹
Björn Lund², Billy Fälth²
Peter Voss³
Jari Puttonen⁴
Jouni Saari⁵
Pekka Heikkinen⁶

- ¹ VTT Technical research Centre in Finland Oy
² Uppsala University
³ Geological Survey of Denmark and Greenland
⁴ Aalto University
⁵ ÅF Consult Oy
⁶ Institute of Seismology, University of Helsinki

Abstract

De-aggregation of probabilistic hazard assessment (PSHA) results show that the dominating source of vibrations with engineering significance to NPP safety is from mid-magnitude earthquakes located at close distances to the plant. This region is called the “near-field” and is known for its particularities when compared to “far-field”. For example, significant duration of the ground motions is shorter, corresponding to S-wave and surface wave arrivals; there are distinctive high velocity peaks in the ground motions and vertical shaking components may exceed horizontal components. These particularities are known to have design consequences, but are often overlooked by engineering codes.

In Fennoscandia, near-field observations of larger magnitude ($M > 3$) earthquakes are missing, and modelling is the only way to supplement the existing empirical data underpinning the attenuation equations in the PSHA studies.

In the ADdGROUND project, during the financial year 2015, we confirmed the near-source effect in small magnitude earthquake recordings in Finland and developed modeling skills and tools to generate synthetic near-field accelerograms starting from process of the fault rupture. We calibrated models with the very few existing near-field measurement cases of small earthquakes. In this report we also highlight some of the potential design consequences of near-source earthquakes to nuclear installations. The consensus seems to be that the destructive potential of these types of earthquakes is generally low. However, they can produce surprisingly larger acceleration values in the range of high frequencies, and can generate high strain rates in the loaded structures and components. In nuclear installations, with stiff components the effect of high frequency shaking should be carefully considered.

Within the ADdGROUND activity we organized two workshops, one on the 8th May 2015 in Espoo, and the second in Copenhagen (15th December 2015). The outcomes have been presented to the nuclear community in the Nordic countries in the NKS Seminar “Nordic perspectives of Fukushima: Where are we now and where do we go? Joint NKS-R and NKS-B Seminar” in Stockholm (12-13.01.2016).

Key words

nuclear power plant safety, earthquake, near-field effects, fault source modeling

NKS-363
ISBN 978-87-7893-448-2
Electronic report, May 2016
NKS Secretariat
P.O. Box 49
DK - 4000 Roskilde, Denmark
Phone +45 4677 4041
www.nks.org
e-mail nks@nks.org

MODELLING AS A TOOL TO AUGMENT GROUND MOTION DATA IN REGIONS OF DIFFUSE SEISMICITY – Progress 2015

Final Report from ADdGROUND Contract: NKS-R_2015_113

Ludovic Fülöp¹, Vilho Jussila¹
Björn Lund², Billy Fälth²
Peter Voss³
Jari Puttonen⁴
Jouni Saari⁵
Pekka Heikkinen⁶

¹ VTT Technical research Centre in Finland Oy

² Uppsala University

³ Geological Survey of Denmark and Greenland

⁴ Aalto University

⁵ ÅF Consult Oy

⁶ Institute of Seismology, University of Helsinki

Table of contents

	Page
1. Introduction	3
2. The sources of hazard for nuclear power plants (NPP's)	4
3. Possible design significance of near-field earthquakes	9
4. Near-source effect in small magnitude earthquake recordings in Finland	13
5. Design implications for stiff structures	24
6. Rupture and ground motion modelling	27
7. Conclusions	32
8. Acknowledgements	32
9. Disclaimer	33
10. References	34

1. Introduction

In Finland, the review of seismic safety of nuclear power plants started in 2011 within the SAFIR2011 program. This activity was launched in preparation for the planning phase of the new units, following a longer break. The intention was to carry out a review of newly emerged seismic data, update the methodologies and create background information for the upgrade of the YVL guides. It was also intended that the work would integrate expertise from theoretical seismology, probabilistic seismic hazard assessment (PSHA), design of nuclear structures and qualification of components. We embarked on activities to increase the communication, and improve its quality, at the seismology / engineering interface, a crucial interface to produce risk relevant seismology studies for nuclear applications. According to this goal the work started in 2011 in a broad consortium including VTT, Aalto University, University of Helsinki, ÅF-Consult LTD and Uppsala University.

The Fukushima Daiichi nuclear disaster struck in the middle of our first work year. While closely following this accident and its regulatory consequence the European stress tests, it became clear that few if any technical lessons may be applicable in Fennoscandia, one of the most stable, low seismicity continental regions. However, one important general lesson was that it is a correct decision to dedicate resources to high-impact low-probability events like earthquakes, even in Finland. Especially since the low likelihood of occurrence often leaves societies under-prepared, while even minimal mitigating actions would result in important improvements. Certainly this “lesson” was understood. Seismic hazard assessments studies were initiated by Fennovoima and TVO/Fortum, for the plant design lifespan. In addition, both in Finland and in Sweden there is a need to better understand post-glacial faulting and its consequences for the much longer waste repository design lifespan.

The outcomes from the SAFIR2011 work were a larger set of newly collected seismic data from Finland and Sweden (the SESA database), a proposal for a ground motion prediction equation or GMPE based on this data, identification of the dominating source of hazard by means of de-aggregation of PSHA results, the quantification of uncertainty in the vibration of building floors and the estimation of damping to be used for stiff concrete structures.

It was the de-aggregation results which triggered the work carried out partly in NKS/ADdGROUND and partly in SAFIR2014/NEST. De-aggregation results showed that the dominating source of ground motions with engineering significance to plant safety comes from mid-magnitude earthquakes located at close distances to the plant. In earthquake engineering, this region is termed the “near-field” and is known for its particularities when compared to “far-field”. Significant duration of the ground motions is shorter, corresponding to S-wave and surface wave arrivals; there are distinctive high velocity peaks in the ground motions and vertical shaking components may exceed horizontal components, while they are about 2/3 in the far-field. These particularities are known to have design consequences, but are often overlooked by engineering codes focusing on far-field events.

Hence, because of the relative importance of the near-field and the lack of measurements in this range in Fennoscandia, we embarked on modelling the ground motions in the vicinity of the epicentres, starting with a model of the fault itself. Such models are associated with large uncertainties, especially in the range of higher frequencies. In 2015 we worked on finding suitable calibration events, collect data from these events and undertake some exploratory modelling. The preliminary findings are reported here. Two workshops were also organized in 2015 to support the work of the project (see Appendix A).

2. Sources of hazard for nuclear power plants (NPP's)

The de-aggregation of the earthquake hazard for certain locations in Finland was carried out in the SAFIR2014/SESA project (Malm and Saari, 2014; Fülöp et al., 2015).

Some key findings are reproduced in Figure 1. The plots give the most probable sources of ground motions with engineering significance arriving to the foundation of a nuclear plant. On the vertical axis is the probability density and on the horizontal axes earthquake magnitude (M) and epicentre distance (D). So peaks in the plot mean that the particular combination of M and D is an important contributor to the hazard. The integration of the plot with M and D is equal to 1. The example location is Pyhäjoki (municipality of Finland and planned location for nuclear power plant), but qualitatively similar plots were obtained for other locations.

The plots are for peak ground acceleration (PGA), spectral acceleration (SA) at 4Hz and spectral acceleration at 10Hz. The spectral acceleration of 4Hz roughly corresponds to the main horizontal vibration mode of a stiff shear-wall type building (e.g. a reactor building). The 10Hz spectral acceleration correspond to the, conventionally accepted, highest amplification factor of the design SA spectra used of NPP's in Finland given in the YVL guides (YVL 2.6, 2001, YVL B.7, 2013). The spectrum is reproduced in Figure 2. It can be seen that the peak-ground acceleration is normalized to $PGA=1m/s^2$ in this plot. The spectra peaks at 10Hz and it assumes a peak amplification of $2.2\times PGA$ at this frequency. The spectral amplification in the vicinity of the usual first horizontal mode of a stiff NPP building (3-4Hz) is about $1.3\times PGA$. This frequency is important, because the first horizontal mode will control the “swinging” of the structure. Hence, the on higher floors the vibration will be amplified significantly in this frequency. The frequency of 10Hz and above affects stiffer equipment and have modes in that range.

The plots in Figure 1 should be read together with the general shape of the spectra from Figure 2 as follows. For a $PGA=0.05g$ one can expect a spectral amplitude of about $SA_{4Hz}\sim 1.3\times 0.05g=0.065g$ and $SA_{10Hz}\sim 2.2\times 0.05g=0.1g$. Similarly for $PGA=0.1g$ one can expect $SA_{4Hz}\sim 1.3\times 0.1g=0.13g$ and $SA_{10Hz}\sim 2.2\times 0.1g=0.22g$ etc. Therefore the pictures in Figure 1 should be read in vertical groups. E.g. Figure 1.b gives the probable sources of a $PGA=0.1g$ shaking, together with the source for the two key frequencies of the spectra at 4Hz (Figure 1.e) and 10Hz (Figure 1.h). As can be seen in the three plots the range of interest is between $M=2..5$ and $D=1..60km$, where large peaks of probabilities are found for target of $PGA=0.1g$. The situation varies a little with the target PGA level, somewhat broader range of M and D corresponding to $PGA=0.05g$ and somewhat narrower to $PGA=0.4g$. These PGA values cover the acceleration targets of design interest in Finland.

One note to the discussion above is that the de-aggregation has been carried out with the probabilistic seismic hazard model where source zones had a largest possible magnitude (M_{max}) defined. Except for the Northern Caledonides source zone, more than 500km away from Pyhäjoki, the highest magnitude was $M_{max}=4.9$ (Fülöp et al., 2015), corresponding to the cut-off in magnitudes in the Figure 1 plots. If larger M_{max} would be allowed, than probably the plots would extend towards the new M_{max} and towards larger distances. It is not within the scope of this work to discuss the M_{max} choices, which are the subject of some debate, rather to point out the possible effects of this parameter.

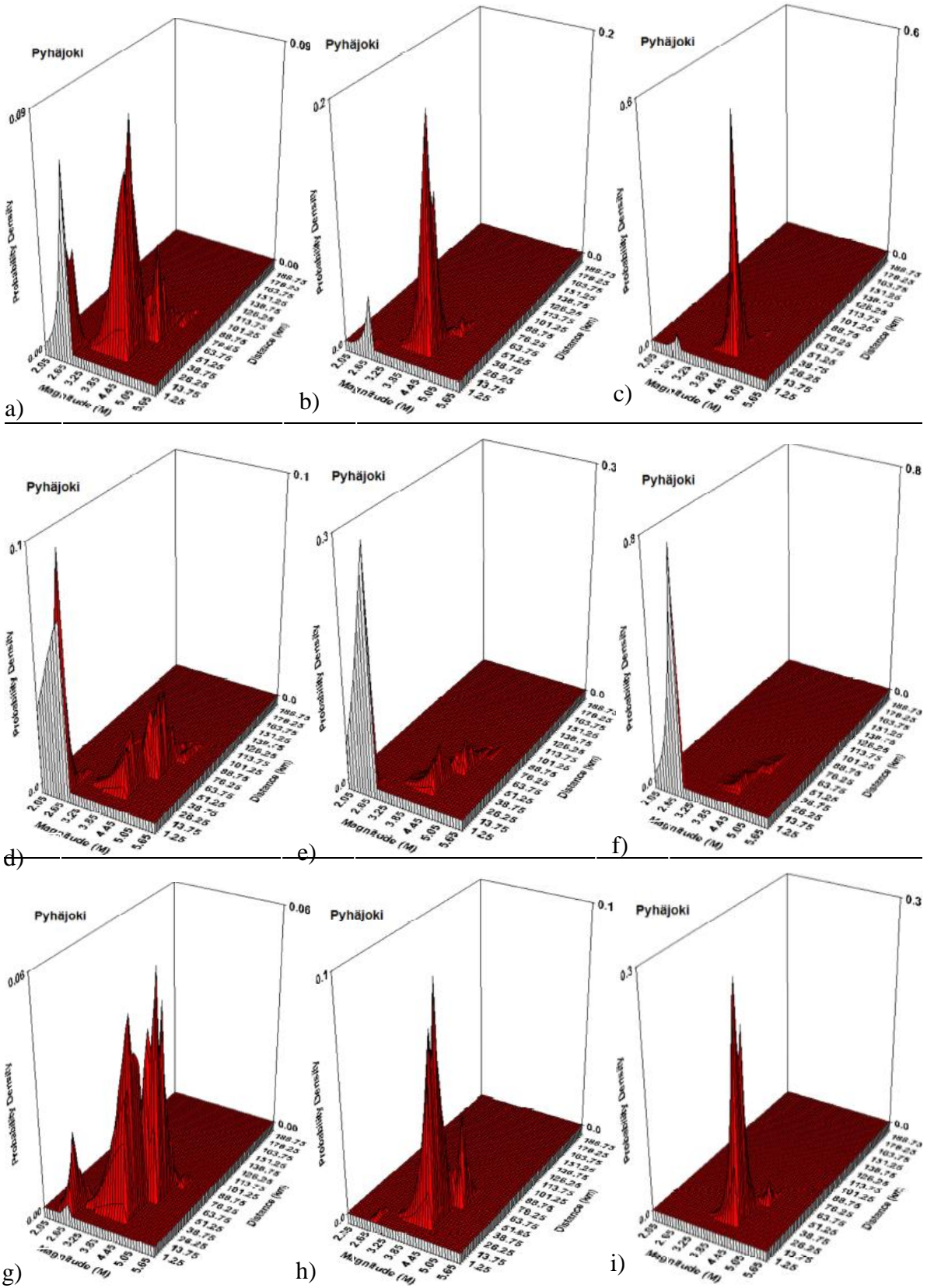


Figure 1. EZ-FRISK magnitude-distance de-aggregation for Pyhäjoki, 5 % damping, average horizontal component of PGA amplitude (a) 0.05g, $M_{\text{mean}}=4.1$, $D_{\text{mean}}=29\text{km}$, (b) 0.1g, $M_{\text{mean}}=4.3$, $D_{\text{mean}}=24\text{km}$, (c) 0.2g, $M_{\text{mean}}=4.4$, $D_{\text{mean}}=21\text{km}$; 4Hz spectral amplitude for (d) 0.05g, $M_{\text{mean}}=3.8$, $D_{\text{mean}}=34\text{km}$, (e) 0.1g, $M_{\text{mean}}=3.6$, $D_{\text{mean}}=22\text{km}$, (f) 0.2g, $M_{\text{mean}}=3.2$, $D_{\text{mean}}=11\text{km}$; and 10Hz spectral amplitude for (g) 0.1g, $M_{\text{mean}}=4.3$, $D_{\text{mean}}=40\text{km}$, (h) 0.2g, $M_{\text{mean}}=4.4$, $D_{\text{mean}}=33\text{km}$, and (i) 0.4g, $M_{\text{mean}}=4.4$, $D_{\text{mean}}=26\text{km}$,

The second note is that for very small distances the use of the attenuation equations in the probabilistic seismic hazard assessment (PSHA) can be problematic. In fact in the original PSHA software, there were already features to deal separately with the region very close to the epicentre (McGuire, 1976). A fixed, or a magnitude dependent limit could be defined for limiting the intensity parameter (e.g. PGA) in the region about 10km or closer.

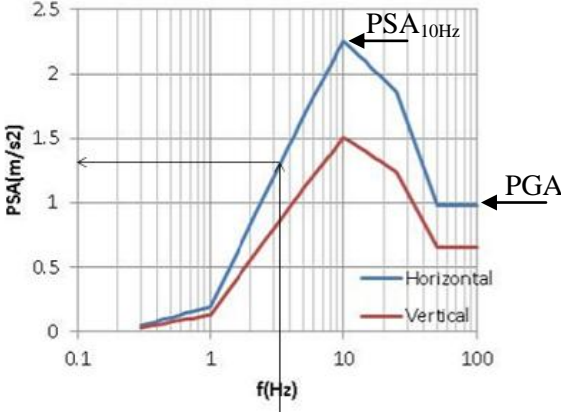


Figure 2. Shape of design spectra for Finland by the YVL guides, developed primarily for southern Finland. Spectral amplification at 3-4Hz is about 1.3xPGA

From the earthquake engineering point of view sites may be classified depending on the distance from the epicentre as presented in Figure 3. As can be seen, the range of $D < 60\text{km}$ is classified as near-field or intermediate site. “Shallow” crustal earthquakes in Fennoscandia have a hypocentre depth of up to 5km. Earthquakes in Fennoscandia occur down to the depth of about 45 km, with most of them between 5 and 20 km.

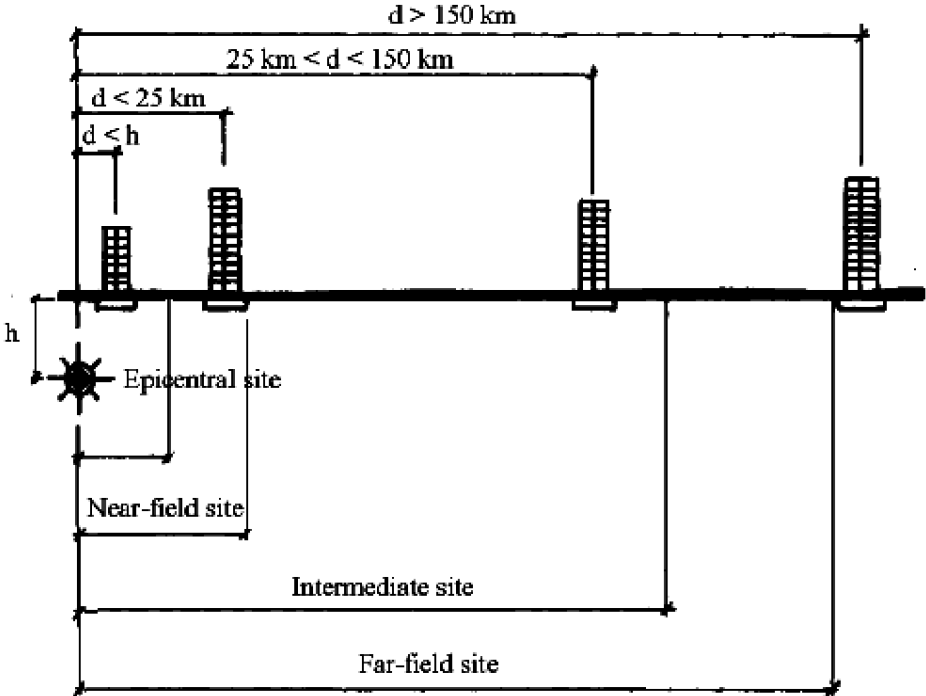


Figure 3. Definitions of different sites depending on the distance (Gioncu and Mazzolani, 2011)

There are known effects related to the regions close to the epicentre. They are firstly related to the proximity of the rupturing fault, which is not of negligible dimension for larger magnitude events. Secondly, they are related to arrivals of the different waveforms as they travel from the

source/fault to the site. Since the different seismic waves have different propagation velocities, at larger distance they arrive with different time delays between each other and overlapping with scattered waves. However, at short distances they arrive with smaller time delays. The main effects, as the epicentre distance is reduced, are that (1) significant duration of the shaking is reduced, (2) higher-frequency shaking is present in the signal, (3) vertical shaking components may be larger than horizontal components, (4) loading is not in repeated cyclic shaking but a few high velocity pulses (Figure 4). Most of these effects are generated by the direct incoming waves, which control the shaking in the vicinity of the epicentre.

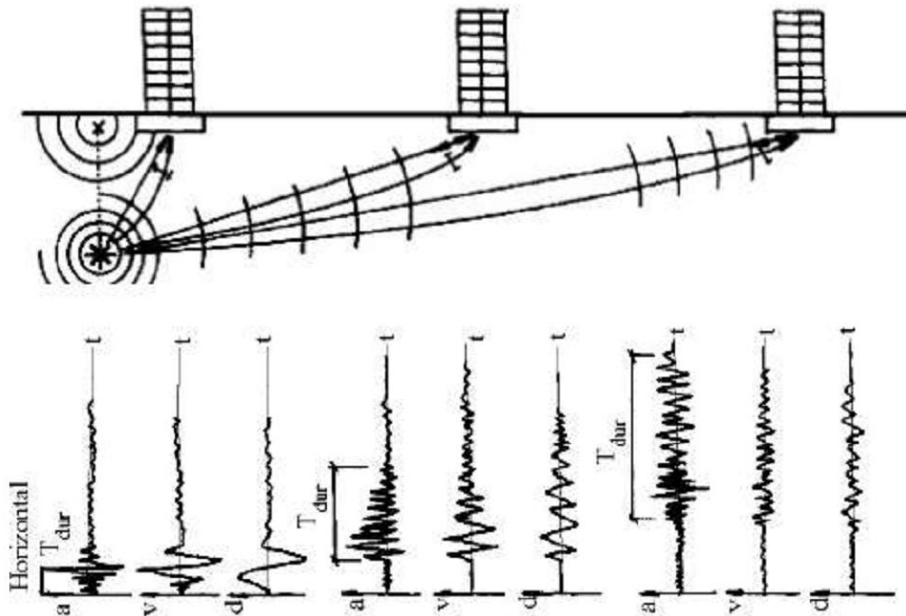


Figure 4. General effect of distance (increasing from left to right) on the observed shaking as accelerations (a), velocities (v) and displacement (d) (Gioncu and Mazzolani, 2011)

With larger magnitudes, and hence fault sizes, the effect of directivity is more easily observed in near-source regions. Once the rupture initiates at the hypocentre, the rupture propagates along the fault. Rupture propagation is influenced by the presence of asperities, the presence of barriers and the geometry of the fault (e.g. curved or stepping faults). Since the rupture velocity is in the range of the propagation velocity of the shear waves, for an observer located in front of the advancing fault rupture, waves generated in the stages of fault rupture arrive in the same instance. Therefore, the simultaneously arriving waves create high peaks of acceleration and velocity in these locations, called forward-directivity regions. Forward directivity locations at certain distance from the fault experience accelerations higher than e.g. sites located lateral to the fault. Part of the 1995 Kobe earthquake's destructiveness was associated to the main city areas being located in the forward directivity of fault rupture (Gioncu and Mazzolani, 2011).

It is also important to distinguish between fault-normal (FN) and fault-parallel (FP) ground motion recordings. The situation is not simple, because analysing a structure to fault-parallel and fault-normal recordings does not ensure that the largest value of an engineering design parameter is captured. The maximum direction (MD) ground motion, leading to peak linear responses of a single degree of freedom system, can correspond to other than the FN and FP directions. However, it is recommended that a structure is analysed to recordings rotated to FN and FP directions, and also MD direction, within a distance range of up to 15km from a fault (Kalkan and Reyes, 2013; Juan Carlos Reyes, 2015).

Directivity and recording direction are source of significant uncertainty in attenuation equations, where the main parameter controlling the vibration amplitude is the distance from the epicentre, hypocentre or fault.

Some of the above effects are advantageous in the design of structures. E.g. the presence of only a few loading cycles makes the shaking less damaging. Hence, near-field earthquakes are regarded to have lower damage potential. Other effects may be disadvantageous. E.g. the higher loading velocity may induce unexpected failure modes in material. It is certain that the study of these effects is necessary in light of the prevailing hazard sources.

3. Possible design significance of near-field earthquakes

While in some cases damage to NPP's have been encountered as a result of shaking from earthquakes, serious accidents like loss of containment of nuclear material has not occurred (Connor et al., 2009). In the case of the Tohoku-Oki earthquake in 2011, the meltdown and near melt down of the reactors at the Fukushima Daiichi and Fukushima Daini NPP's were due to failures in backup power systems caused by the tsunami, and not by the shaking caused by the earthquake. At both plants the reactors were automatically shut down immediately after the earthquake.

Nonetheless impact of earthquake shaking has been of serious concern in a number of cases, e.g. at the Kashiwazaki-Kariwa nuclear power plant. On July 16, 2007 a M6.8 earthquake occurred 16km offshore of the Kashiwazaki-Kariwa NPP, the largest power station in Japan. The plant performed well, with limited damage and a few minor releases of radioactivity to the environment. The real surprise was that the event exceeded the seismic hazard guidelines, calling in question the data for the modelling of the hazard and the modelling method itself (Connor et al., 2009).

The assessment and classification of three faults 20-40km from the site as inactive turned out to be incorrect. It was also observed/concluded that, when earthquakes are located a few km from the sites, source parameters such as fault mechanism and directivity effects may play an important role in impacts. With the dense seismic network of Japan, the number of near-field recordings increased, with these recordings often showing larger than expected accelerations when compared to the values used in attenuation relationships.

As an outcome of the safety review, the IAEA team recommends that: *“The attenuation relationships to be used for faults in the near region should include both empirical methods based on observed seismic data as well as analytical methods producing synthetic seismograms compatible with the fault mechanism and the travel path. It is expected to be able to address directivity issues using this methodology”* (Preliminary findings and lessons learned from the 16 July 2007 earthquake at Kashiwazaki Kariwa NPP - The Niigataken Chuetsu-Oki Earthquake (Volume I), 2007). These conclusions were confirmed in the follow-up reports of the IAEA: *“When there are significant contributions to the seismic hazard by active faults in the site vicinity or the near region, source parameters such as the fault mechanism and directivity effects may play an important role. This may cause variations in the hazard even within areas very close to each other.”* (Follow-up IAEA Mission in Relation to the Findings and Lessons Learned from the 16 July 2007 Earthquake at Kashiwazaki-Kariwa NPP - Volume I, 2008). Site vicinity is defined as 5km radius around the plant, while near-regional as an area not less than 25km by the IAEA Safety Guide NS-G-3.3 (IAEA, 2002).

For NPP structures as early as in 1980's, besides the general far-field accelerogram, it is recommended to postulate a near-field earthquake of small magnitude, shallow focal depth and short/3s duration of strong motion. This earthquake will typically affect a radius of 5-15km, will have high frequency content (4-8Hz) and exceptionally high acceleration spikes (0.4-0.7g's); accelerations strongly depending on the characteristics of the causative faults (Constantopoulos et al., 1980). Seismic re-evaluations in the nuclear context were showing vertical shaking components, from small near-field earthquakes, to exceed shaking from much larger far-field events in the range of frequencies above ~5Hz, on soil (Kostov, 2001). And it

was noted that near-field earthquakes with small to moderate magnitudes can result in significant PGA's, controlled by higher frequencies. Significant structural damage is unlikely from high-frequency shaking components, but they may affect instrumentation and control systems (Labbé, 2001).

As a result of unexpected accelerations recorded, among others during the Kobe earthquake of 1995, a new Beyond Design Basis earthquake level has been introduced in Japan (S_s), and in the US (Stevenson, 2014), with S_s acceleration defined as 1.67 times that of the Safe Shutdown Earthquake (SSE). The accepted performance for the Beyond Design Basis earthquake extends to post-elastic strains in the material either directly, or by proposing inelastic energy absorption factors F_{μ} (ASCE, 2005)., as one feature of the near-field shaking is to limit inelastic response.

The Nuclear Regulatory Authority (NRA, 2013) guidelines also contain provisions for considering ground motions without information on a specific fault. The requirements cover the situation of undetected faults not extending to the ground surface (orphan fault), within the seismogenic layer, generating an earthquake at an unforeseen location. This scenario covers the possibility of near-source earthquakes, with an upper limit of Mw6.5 (in Japan), by instructing the use of data from sixteen such events, which occurred between 1996 and 2013 (NRA, 2013).

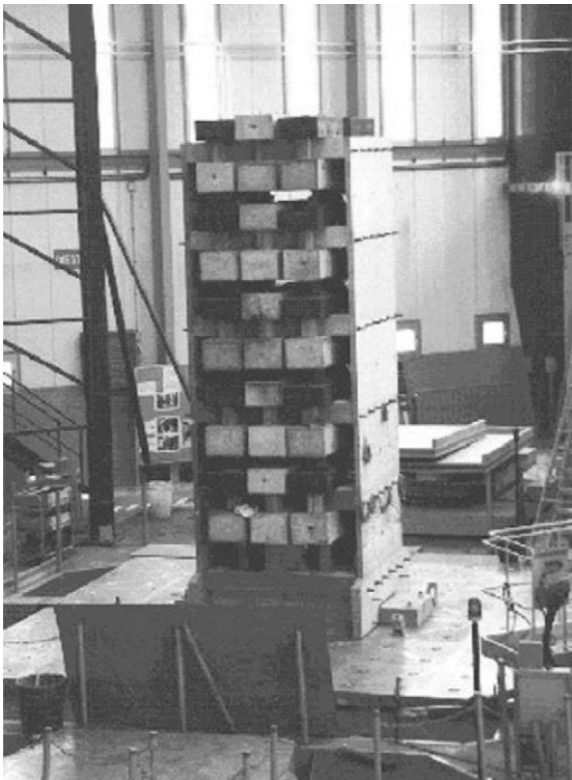


Figure 5. Arrangement of the 5 floor shear wall structure on the shake table (Labbé and Altinyollar, 2011)

Following the observations that small near-field earthquakes can result in large PGA's, controlled by high frequencies, a collaborative project was launched by the IAEA in cooperation with JRC in order to study the safety significance of near-field events to NPP's. The three years activity, with participation from 18 countries is reported by Labbé and Altinyollar (2011). The study included shake table testing of a five floor concrete shear-wall

type structure (Figure 5), to far-field (FF) and near-field (NF) type motions and benchmark calculation in order to replicate the observed behaviour.

The main performance indicators in the study have been the top floor displacement, top floor spectra, and base bending. The authors compare the achieved performance with the one predicted by the established NPP design practice of response spectrum analysis. The primary conclusion of the study is that the damage potential of NF earthquakes is low, despite the large PGA's observed in the free-field measurements. The damage potential in the study means damage of the primary structure, and it is tightly related to the frequency-content of the input signals in relationship with the fundamental frequency of the structure (7.24Hz).

The authors conclude that the distinction of the signals in NF and FF is insignificant, when both can be regarded as high-frequency input motions in relationship to the fundamental frequency of 7.24Hz. During the CAMUS experiments the structure was softening due to localized/small damage. Consequently the fundamental frequency was shifting from 7.24Hz to 5Hz (Figure 6), a shift which was not well replicated by calculations. The small nonlinearities in the structure proved to be very effective means of mitigating the impact of large PGA's of NF signals. The authors suggest that non-linearity should be taken into account in order to predict reasonably realistic floor response spectra (Labbé and Altinyollar, 2011).

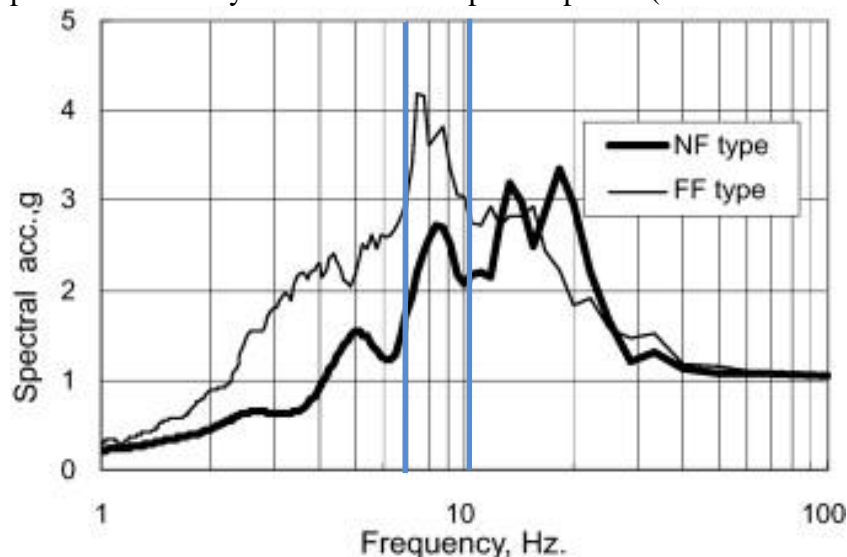


Figure 6. Normalized pseudo-acceleration (PSA) spectra of the NF and FF type shaking considered in the CAMUS study (Labbé and Altinyollar, 2011). The fundamental frequency of the undamaged frame (7.24Hz), and of the damaged frame (5Hz) are highlighted with dashed lines.

The NF/FF distinction is not discussed explicitly when it comes to contributions of the higher vibration modes to the response of structures. This can be attributed partly to the stiff benchmark structural typology, where horizontal vibration is controlled by the fundamental mode. Higher horizontal modes are having small impact on the global response. The situation is contrary to softer traditional buildings, especially moment resisting frames, where NF damage is partly attributed to contributions of the second/third horizontal vibration modes (Huang, 2003; Hall et al., 1995; Gioncu et al., 2014) and partly to high loading velocities (Gioncu et al., 2014).

One note is that vibration of sub-structures of NPP building may be controlled by higher modes of vibration (e.g. vertical vibration of individual floors). In that case the controlling

structural frequency is much larger. This effect can have an impact on qualification of components to NF versus FF shaking.

Labbé and Altinyollar, (2011) argues for a review of the design approach to deal with high frequency inputs, as follows: *Historically, the conventional nuclear approach was established in order to deal with the conventional design situation, which consists of evaluating effects of rather low frequency input motions on stiff buildings such as reactor buildings of nuclear power plants. The conventional nuclear practice (response spectrum method associated to non-exceedance of conventional limit state) was established accordingly. This approach proved to be effective and reliable in the context of a conventional design situation, i.e. situations before the recording of high frequency ground input motions. This approach should be reconsidered when dealing with the type of high frequency inputs considered in this paper* (Labbé and Altinyollar, 2011). The recommendations include (1) high frequency input motions as displacement-controlled loads (2) acknowledging small non-linear effects by linearization techniques or other means of simple nonlinear structural analysis.

A different effect of near-field earthquake is discussed by Gioncu et al. (2014), namely the effect of high velocity loading. The effect of near-source earthquakes is likened to that of an impact received by the building (Figure 7). The consequence of this loading scenario is a much higher strain rate experienced by the structures and components (Figure 8).

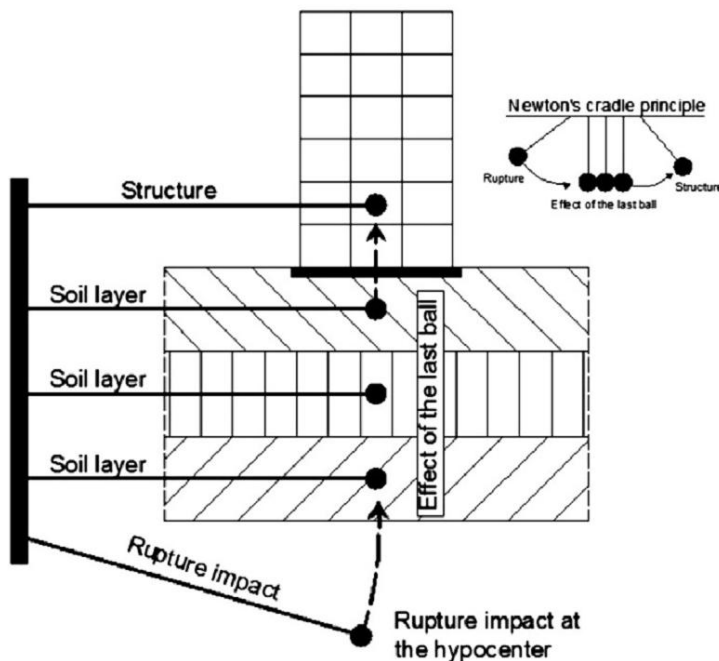


Figure 7. Effect of the fault rupture received by the building as it was the last ball in Newton's cradle (Gioncu et al., 2014)

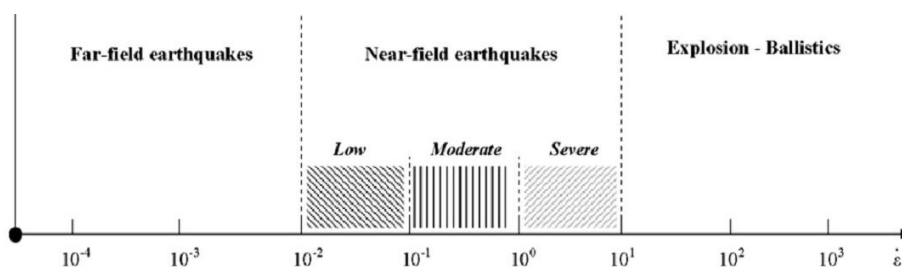


Figure 8. Strain rates (1/sec) from the different loading scenarios, with near-field earthquakes ranging between far-field earthquakes and impact loads (Gioncu et al., 2014)

4. Near-source effects in small magnitude earthquake recordings in Finland

As stated earlier, recordings of strong motions from Fennoscandia are not available (e.g. Near-field, $M > 5.5$). There are recordings of smaller magnitude earthquakes, even at short distances and there are recordings of larger events, up to magnitude $M = 4.9$, at larger distance. A recent update on the available empirical data was published by (Vuorinen, 2015). The map of events for the study is given in Figure 9, while the distribution of the recordings with magnitudes and distances is presented in Figure 10. As can be seen, the recordings for $M > 2$ in the distance range of $D < 60\text{km}$ are quite rare. The data group with reasonable magnitudes for $D < 60\text{km}$, which would allow an estimation of the randomness would be the $2 < M < 3$.

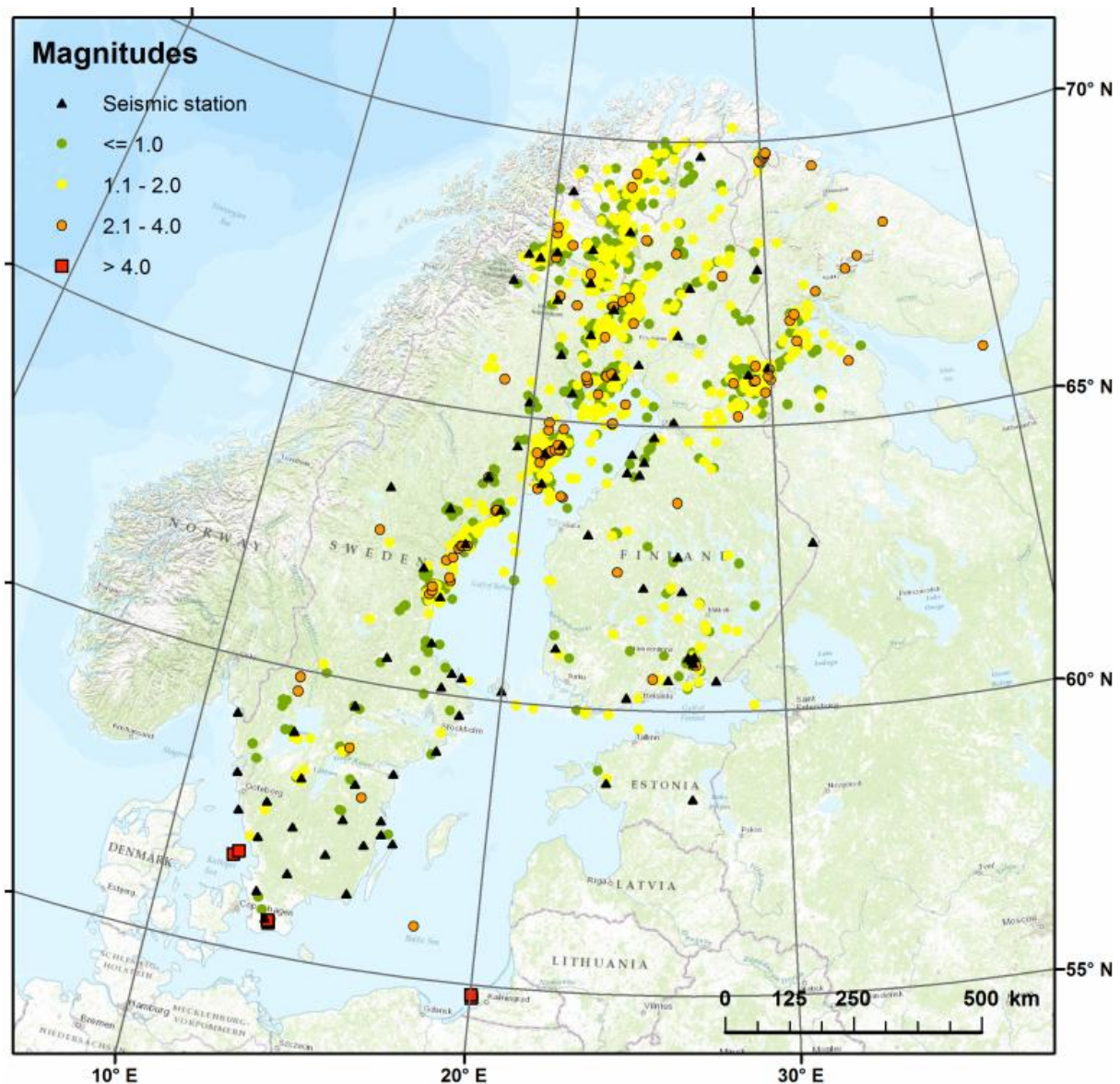


Figure 9. Map of events grouped by magnitude and seismic stations marked with black triangles (Vuorinen, 2015)

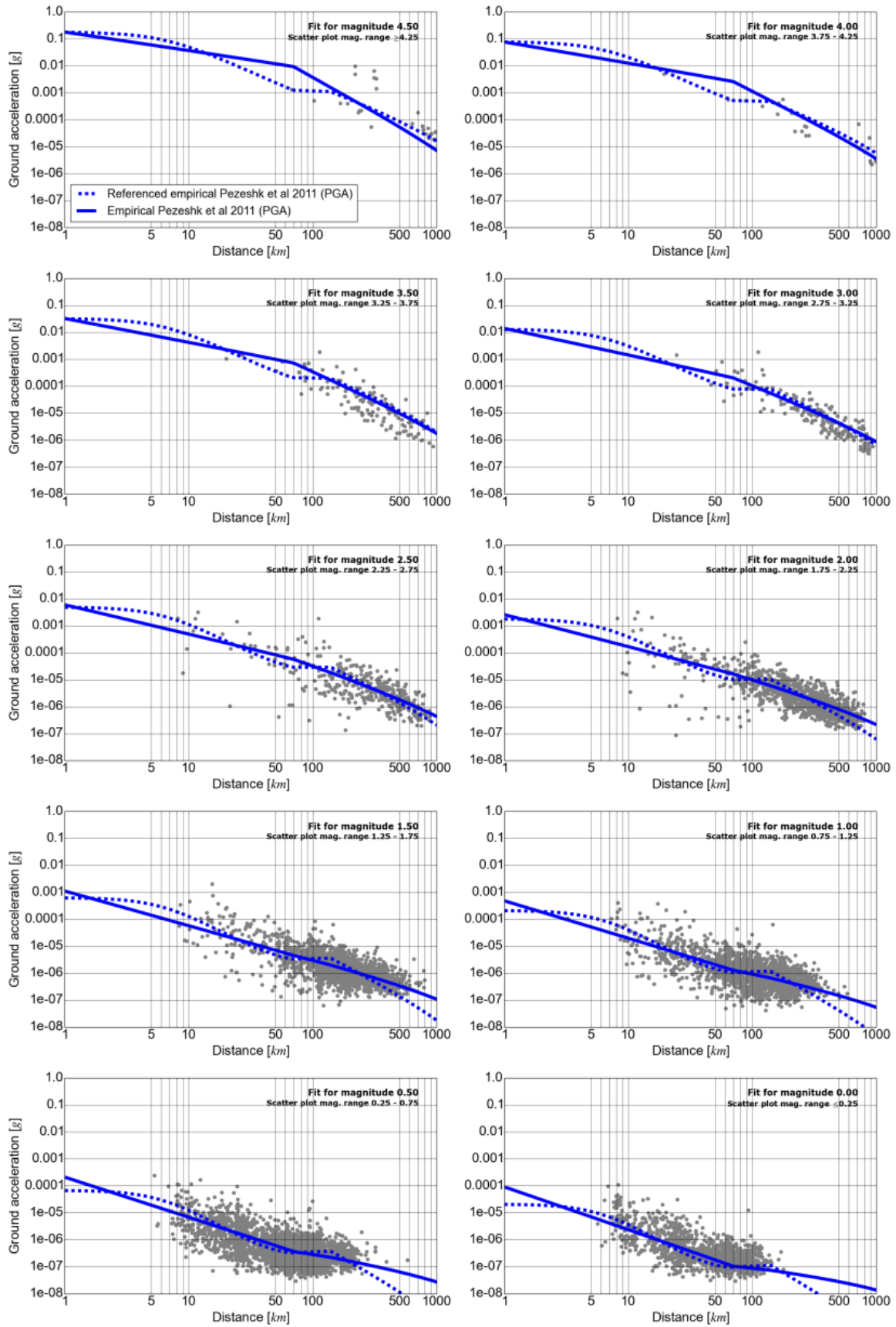


Figure 10. PGA of the recordings in the Vuorinen data matched to attenuation rules from the literature. The figures correspond to bins of magnitude $M=0.5$ (Vuorinen, 2015)

Given this data scarcity we analysed one of the existing data sets from a swarm in Kouvola Southern-Finland, with the largest measured event of $M_L=2.6$. The advantage of this data is that measurements were taken at very close range (2-9km) and the sampling rate was very high, 250Hz. Earlier analysis and data on the swarm has been reported by (Smedberg et al., 2012; Smedberg et al., 2012).

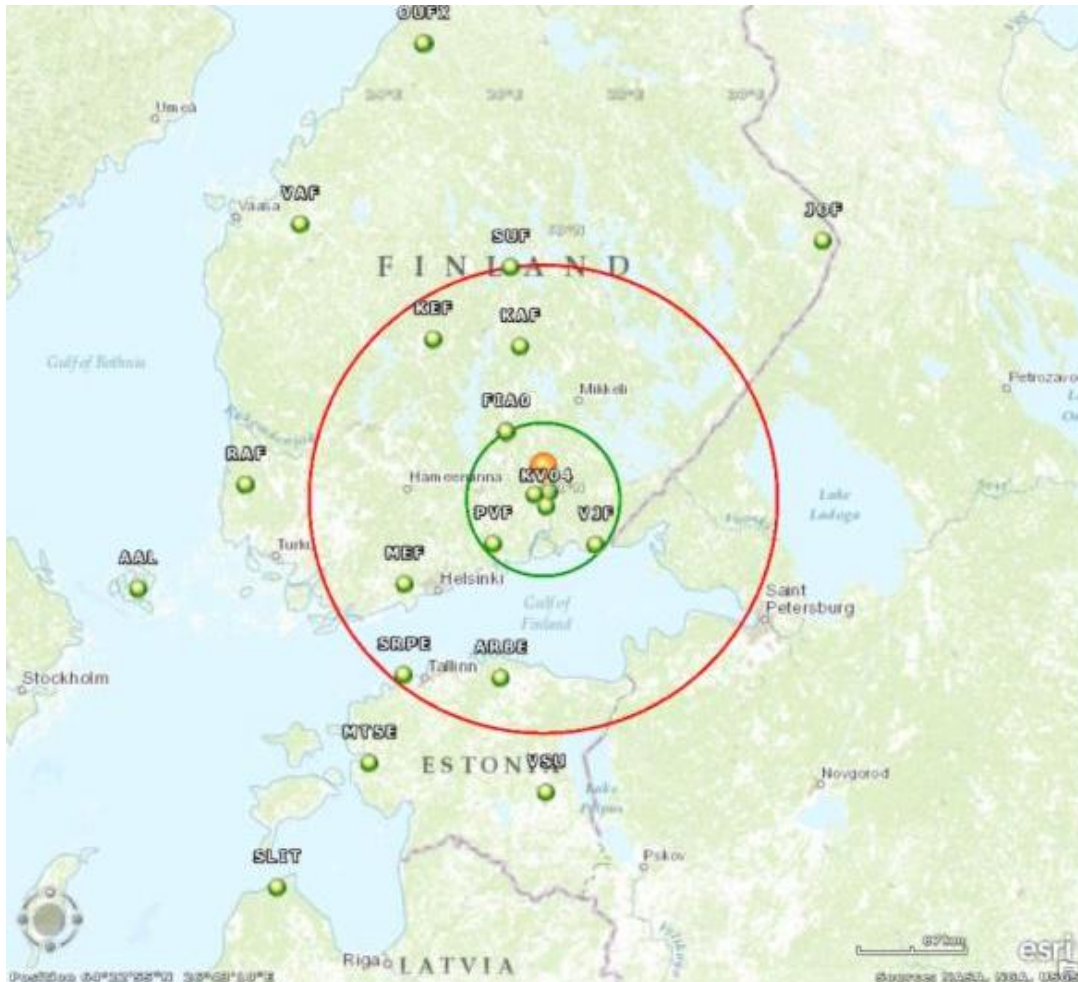


Figure 11. Recordings available of the Kouvola swarm in the National networks of Finland and Estonia. Four temporary stations in the vicinity of the epicentre (orange dot) are called KV and were deployed for the purpose of recording the swarm. The green circle is 70km around the epicentre; the red circle 200km.

The data was imported to SEISAN, a seismic analysis system and a simple database for analysing earthquakes from analogue and digital data (Ottmöller et al., 2014, Havskov and Ottmoller, 1999). Processing of the data has been carried out in SEISAN.

The seismic recordings of one of the Kouvola swarm earthquakes (DEC 22nd 2011 07:22) on the nearby seismic stations is seen in Figure 12. Data are shown in a 35 s long time window. Each trace shows the signal from the vertical component seismic sensor, the station code is given to the left of the signals and the component codes BHZ or SHZ define the used sensor, broad band sensor or short period sensor, respectively. Red markers on the traces gives the arrival times of the pressure wave (P), the shear wave (S) and where the amplitudes are measured (MSG). The I and E associated with the P and S gives whether the phase is impulsive or emergent, respectively. The D or C to the right of the P phase reading gives the first motion of the phase, dilatation or compression, respectively. The numbers in black on the left and right sides above the traces gives the DC level and maximum amplitude of the traces,

respectively. The traces are plotted downward with respect to distance, as distance increases the time-gap between the arriving P and S waves increases due to the different propagation velocity of the two wave types. On the three lower traces the shear wave is clearly separated into a high frequent direct shear wave and a low frequent surface wave part (phase name Rg) 3-4 s later. The signal recorded on the station closes to the earthquake KV01 show a large offset after the recordings of the earthquake. This offset could be a result of a physical displacement of the sensor due to the shaking from the earthquake.

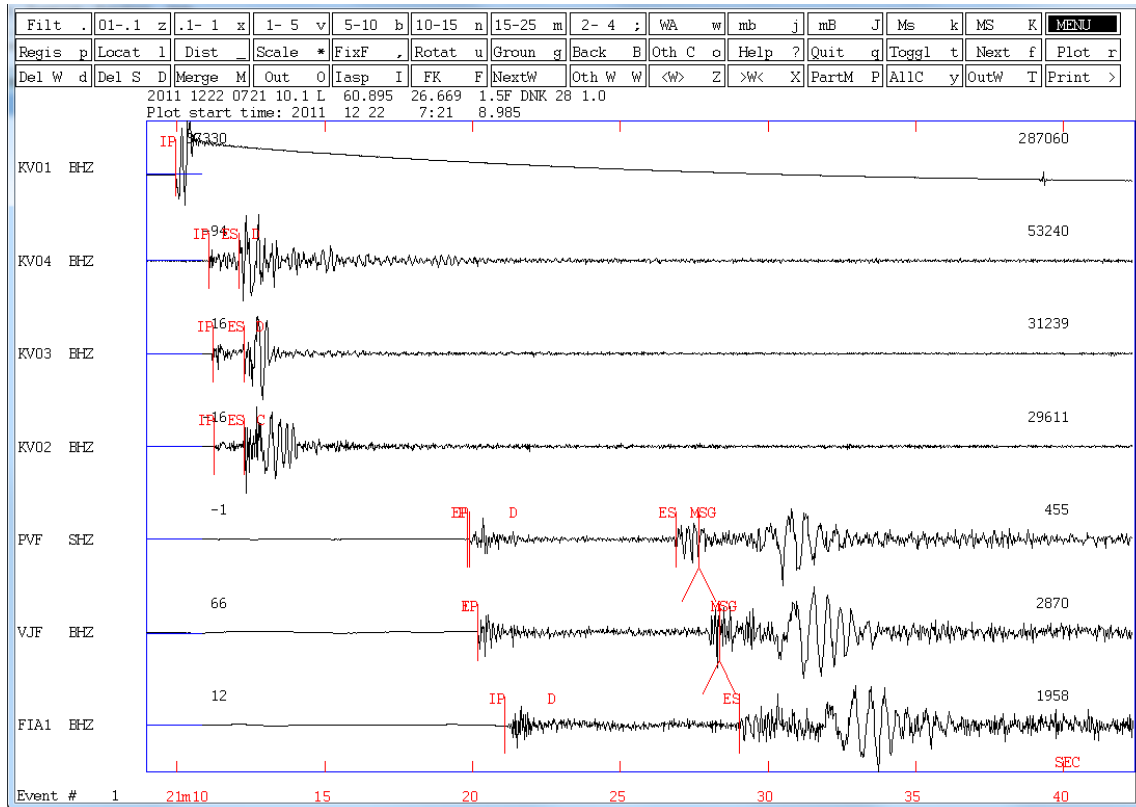


Figure 12. Vertical components only stations closer than 70km, representation in SEISAN. The wave arrival times are marked on the signals. The station distances to the hypocentre KV01 (2km), KV04 (6.5km), KV03 (8.7km), KV02(9.9km), PVF(58.8km), VJF(62.6km) and FIA1 (68.9km).

The fault plane solution for the $M_L=2.6$ event is given in Figure 13. It corresponds to strike angle of $STR=63$ degs, dip angle of $DIP=59$ degs and rake angle of $RAK=118$ degs. A composite fault plane for the three strongest events has been calculated as $STR=216$ degs, $DIP=75$ degs and $RAK=95$ deg and reported by Korja and Kosonen (2015), based on Smedberg et al. (2012).

The two solutions agree on the approximate alignment of the fault (North-East/South West), that the fault is high-angle and that the main movement is reverse dip direction movement. $RAK=+90$ degrees would indicate pure reverse dip direction motion, and the solutions deviate from this only by 5 and 28 degrees, respectively. The two solutions disagree on the strike direction, hence on the dip direction of the fault. In the first model the strike is towards North-East and the fault dips towards South-East, while in the second case the strike direction is South-West, and the fault dips towards North-West.

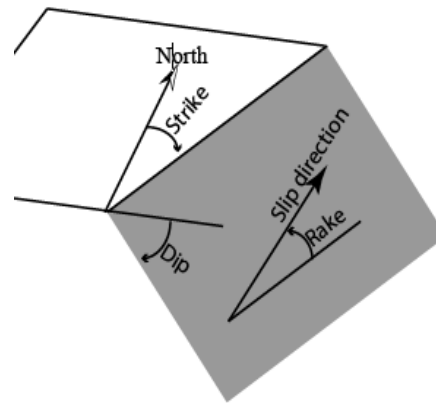
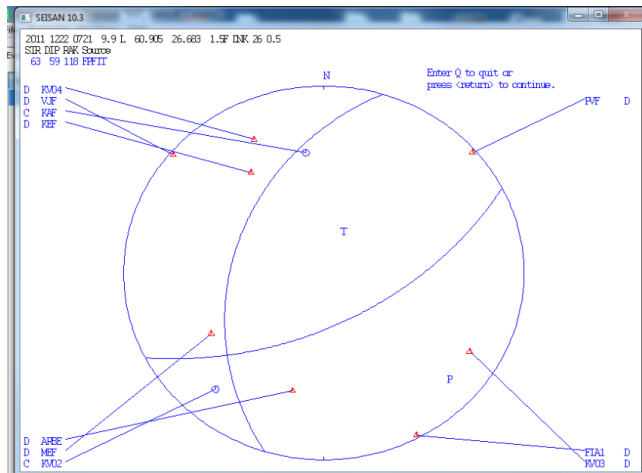


Figure 13. Fault plane solution of the $M_L=2.6$ event from SEISAN, and schematic presentation of the meaning of strike (STR), dip (DIP) and rake (RAK) angles

The KV stations were equipped with Nanometrics Trillium 120PA seismometers and the Nanometrics Taurus digitizers, and had the ability to resolve signal with very low frequency (<0.01 Hz). The signals from the KV stations have been corrected for instrumentation response and converted to acceleration, velocity and displacement. The Fourier spectra of the acceleration signals are given in Figure 14.

In order to understand the source of the high frequency peaks in the Fourier plot, and to get an overview of the noise at the four stations, the power spectral density (PSD) was calculated for each channel in one hour intervals in the time frame of the event. Sample PSD plots for the vertical (z) direction channels are given in Figure 15. KV04 is the noisiest site across all frequencies. Both KV03 and KV04 show clear diurnal variations above 2Hz, which could be due to temperature variations or cultural noise like traffic. In the high frequency band one see a lot of peaks that are consistent during the whole period see e.g. KV04 and KV02 at 20Hz.

A more detailed look on January 11-15 (Figure 16), with one nearby earthquake at 21.18 on 12th of January 2012 and one around 16 o'clock on January 14th, indicate that the earthquakes generate some signals in the high frequency range, but it coincide with cultural noise.

It has been decided to remove the effect of the very high frequency parts, above 50Hz, in the temporary station's signals. Hence, 6th order Butterworth bandpass filter between 0.25-50Hz has been applied to the signals, in order to eliminate the major uncertainties related to the high frequencies and to make the measurements compatible with those from the permanent stations in Finland. Still, the noise level even below 50Hz may be significant in some stations (e.g. at 20Hz in KV02 and KV04), and conclusions retain a certain level of uncertainty. Pseudo-acceleration spectra (PSA) have been generated from the bandpass filtered accelerograms, and are presented in Figure 17.

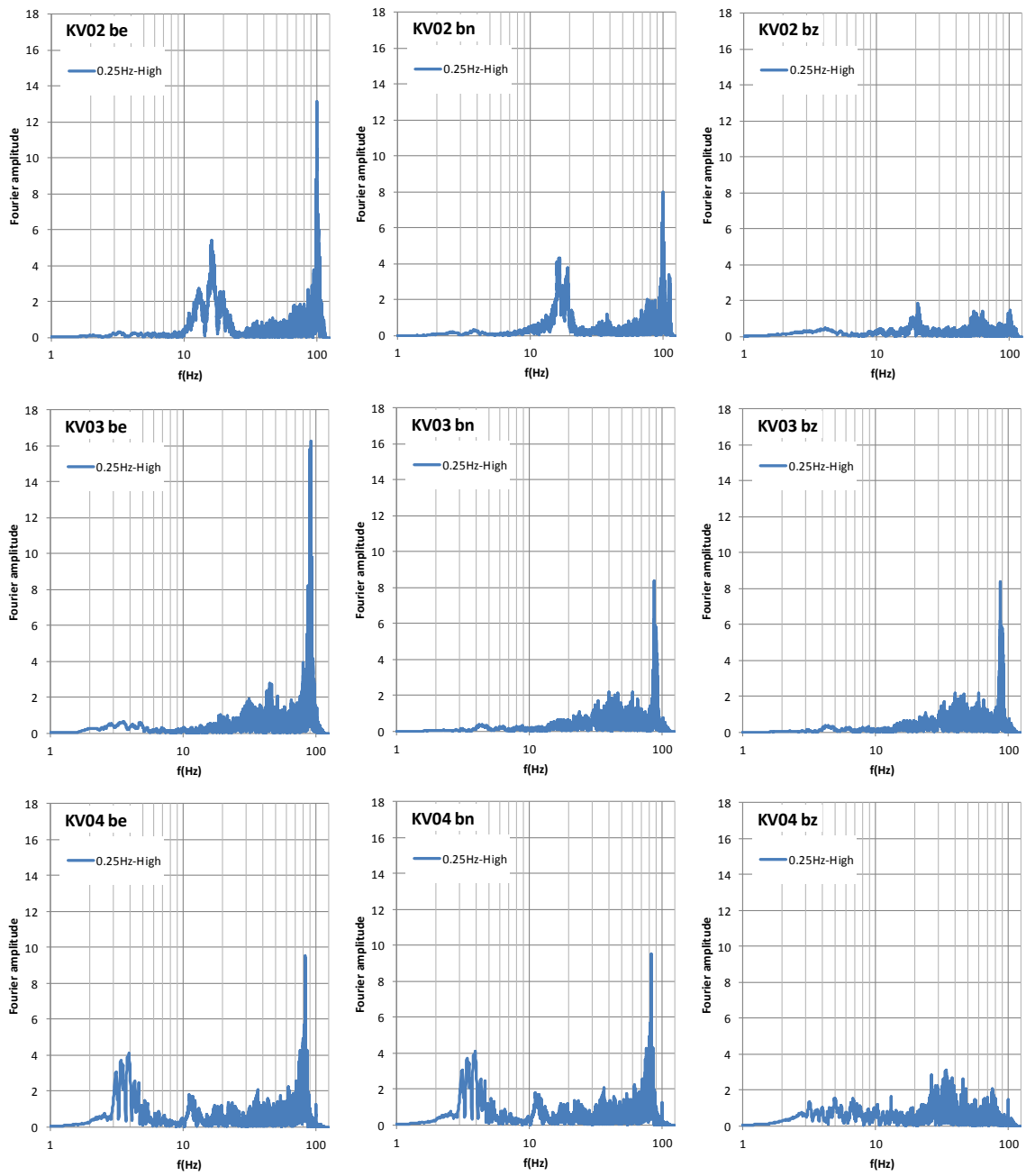


Figure 14. Fourier spectra of the KV02, KV03 and KV04 station acceleration recordings. Blue lines we the signals filtered with Butterworth 6th order high pass filter above 0.25Hz.

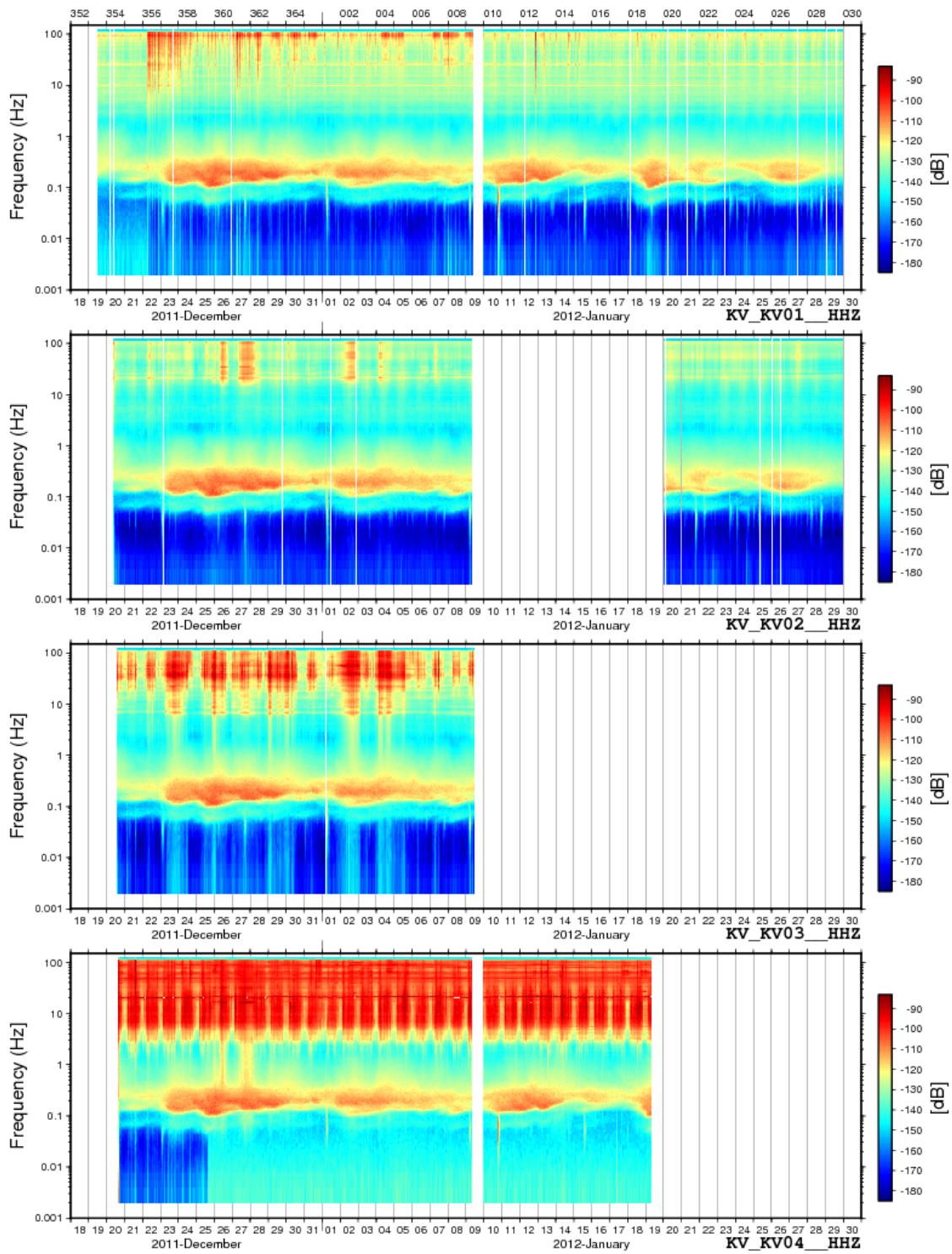


Figure 15. Sample PSD plots for the temporary station’s vertical (z) direction measuring channels: Hourly intervals in 20.12.2011/22.01.2012. From top to bottom the stations are KV01, KV02, KV03 and KV04

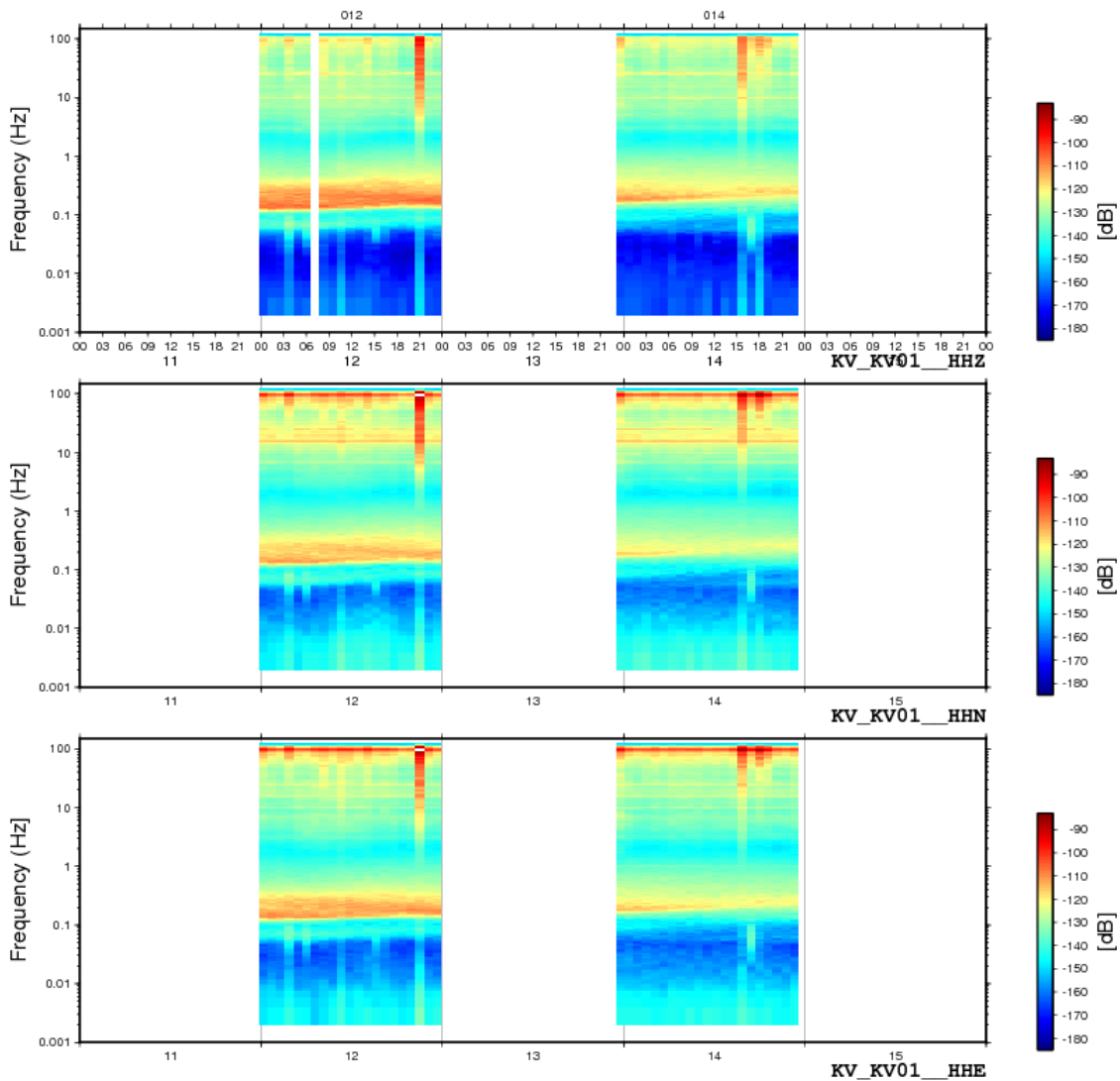


Figure 16. PSD plots for temporary station KV01 all three measuring channels (Vertical/HHZ, North/HHN and East/HHZ). Nearby earthquake events are 21.18 on 12th of January and around 16 o'clock on 14th of January. The increase around 18 o'clock on 14th of January, correlate with some explosions in northern Sweden (<http://www.seismo.helsinki.fi/bulletin/list/pdfbul/hel2012.01>).

There are two curves given in each plot in Figure 17: one corresponding to the band-pass filtered signal between 0.25-50Hz, and a second band-pass filtered between 0.25-25Hz. The purpose of this representation is to highlight the content of the signals in the high frequency range. Traditionally, the cut-off frequencies for strong motion data are 0.25Hz and 25Hz, as used e.g. in the European Strong Motion Database (“Internet Site for European Strong-Motion Data,” n.d.). Since strong motion data is the basis for developing ground motion prediction equations, it was chosen to present the data with compatible band-pass filtering 0.25-25Hz.

Normally, strong motion data is filtered with a low cut-off frequency and a high-cut-off frequency. The low cut-off frequency has an important effect on the long period time domain, especially the peak-ground velocity and ground displacement. The high cut-off frequency removes high-frequency content and may affect the peak-ground acceleration. However, at least for ordinary structures and for applications with structural response primary focus, the frequencies outside the band-pass filter range of 0.25-25Hz are considered not to have significance for safety.

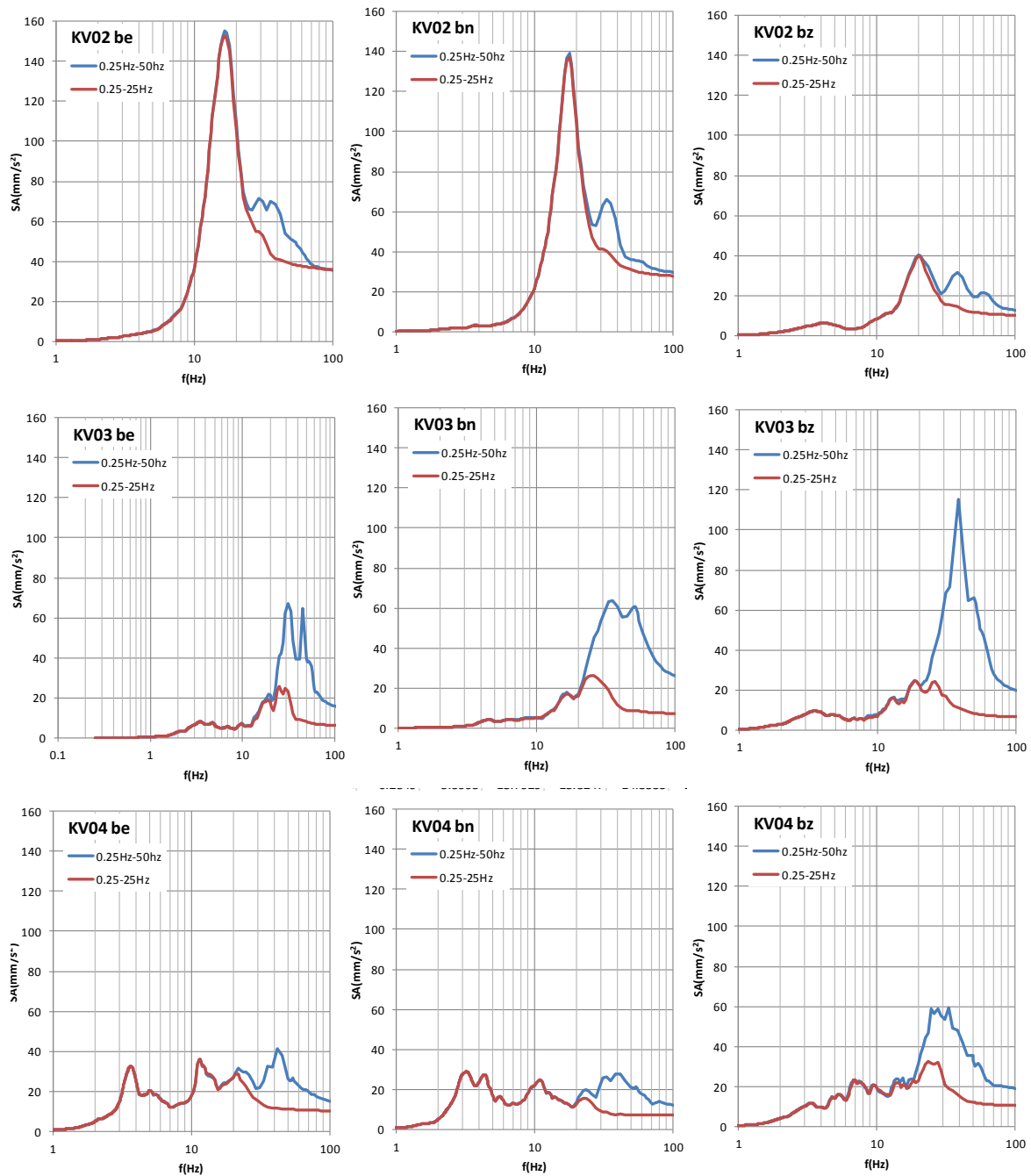


Figure 17. PSA response spectra of the accelerograms in the KV stations. Hypocentre distances are KV04 (6.5km), KV03 (8.7km), KV02 (9.9km). Sampling frequency was 250Hz.

It can be observed that the amplification of accelerations in the high frequency ranges is important for KV03 and KV04. However, the noise content of the station KV04 is very high above frequencies of 2Hz (Figure 15), making measurements of this station questionable.

The above spectral plots should be interpreted together with the information on the immediate vicinity of the epicentre and the location of the installed stations (Figure 18). While we do not have the exact soil data for the station locations, it can be estimated that the amplification at about 15Hz for station KV02, and the amplification at about 3.5Hz for station KV04 are most probably caused by soil effects. KV04 is also surrounded by living quarters, explaining the high level of background noise at this location. Hence, it is station KV03 which is located on bedrock.

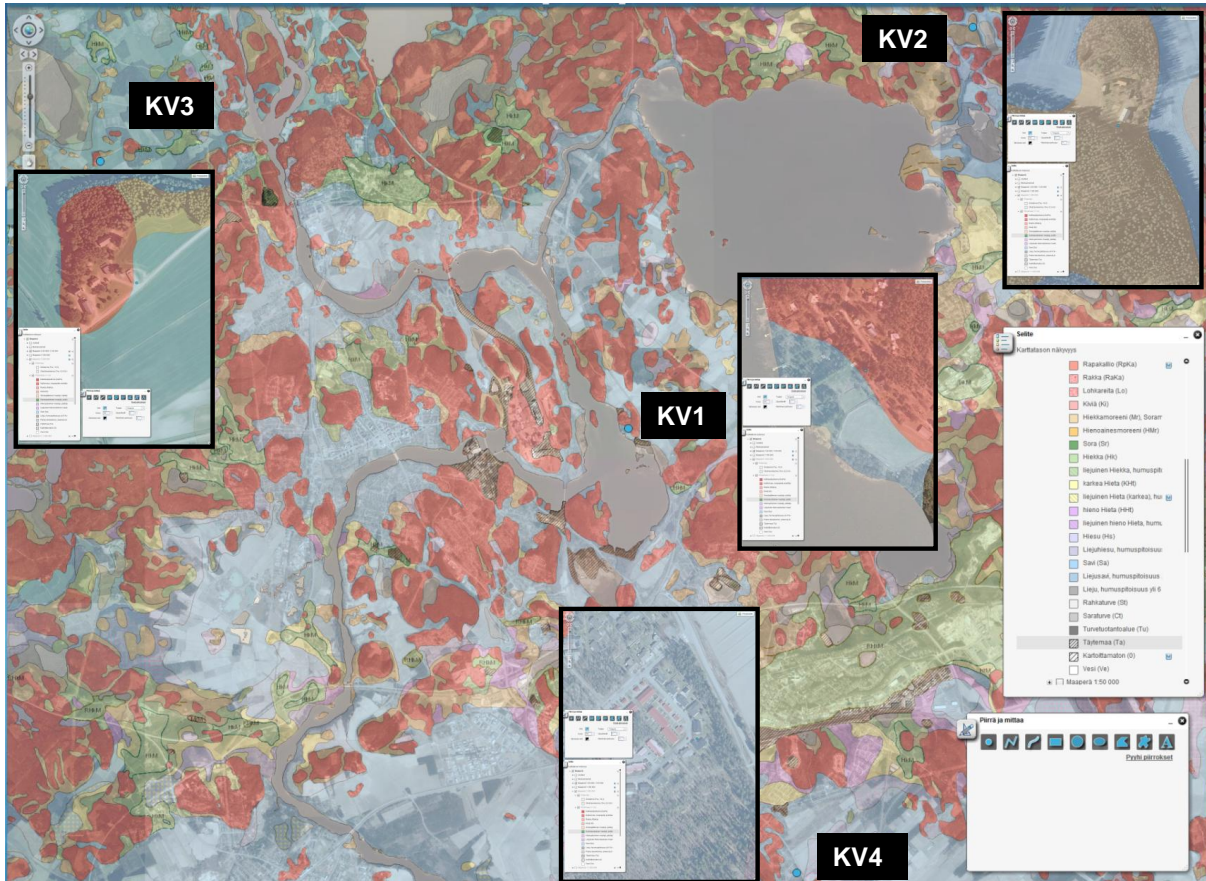


Figure 18. The location of the temporary KV stations as green circle, in relation to the surface layer provided by the Geological Survey of Finland GTK (GTK, 2015). The stations KV1 and KV3 are located on the rock outcrop (red), but stations KV2 and KV4 are located on layers of sandy moraine (yellow) and clay (blue) respectively

Figure 19 presents the PSA spectra of the accelerations measured in the more remote stations KAF, PVF and VJF. These stations are part of the permanent national network and they measure with a sampling rate of 100Hz. They are also located on rock sites.

As is evident from Figure 12 the duration of shaking is more extended at larger distances from the epicentre, as exemplified also in Figure 4. The wave arrivals in station KV01 are so close that it is difficult to separate the different phases.

The measurements at close distance reveal the presence of high frequency content in the signals (Figure 14), which are judged to be reliable up to about 50Hz. Spectra from signals at largest distances have similar features (Figure 19).

The KV station recordings are of limited use, since in some cases, the presence of the soil and associated amplification disturb the interpretation of the signals. We decided that the best course of action is to use the measurements of station KV03 as a reference for the model calibration in the following sections.

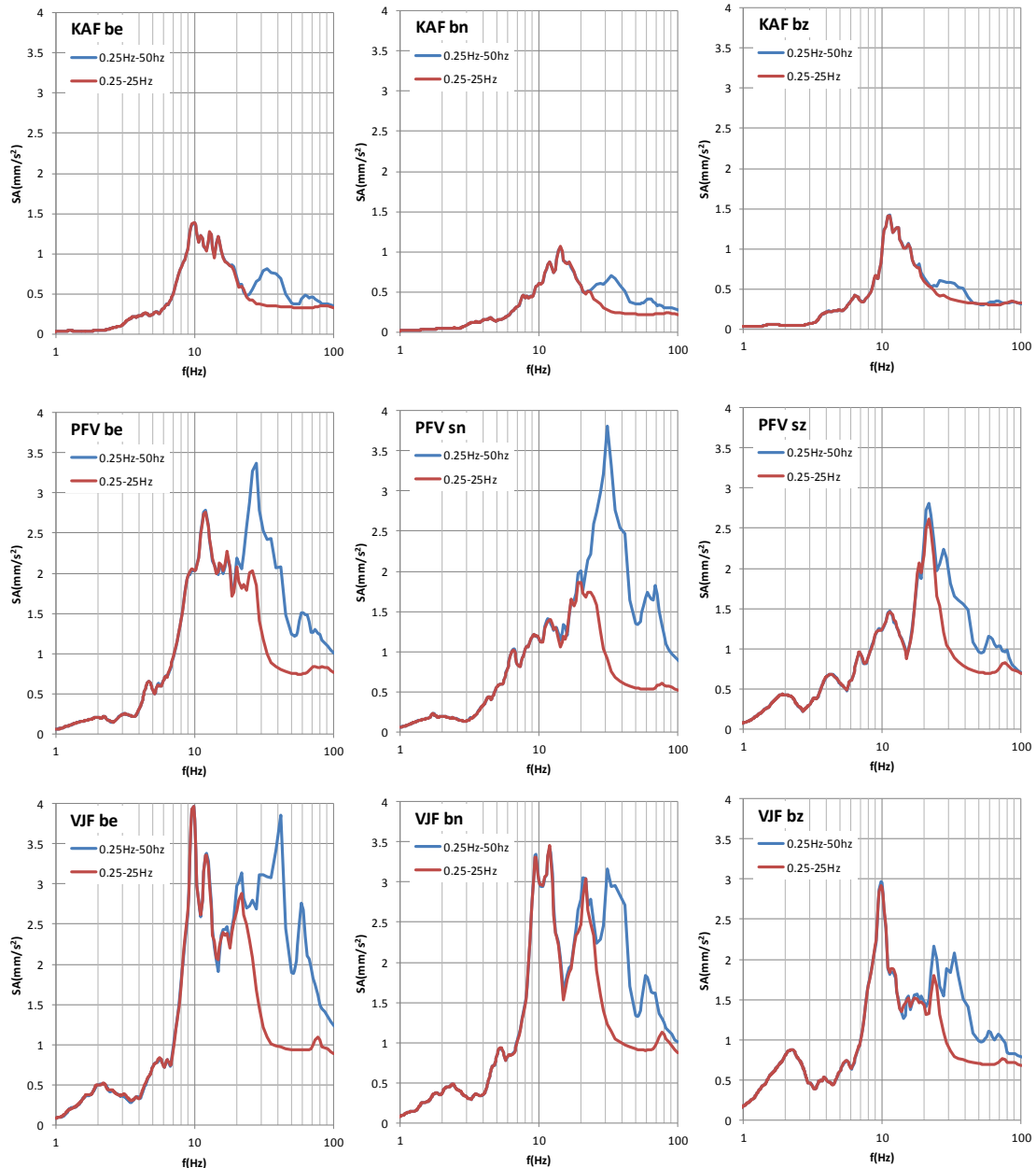


Figure 19. PSA response spectra of the accelerograms at the permanent national network stations KAF(135.4km), PFV(40.3km) and VJF(62.2km). Sampling frequency is 100Hz.

It is interesting to compare the spectra from stations PFV and VJF. If we correlate the positions of the two stations with the North-East/South-West orientation of the fault, it can be noticed that PFV is a site located forward of the fault, while VJF is lateral to the fault (Figure 11). Since the fault-slip in the strike direction is small compared to the dip direction (RAK angles close to 90degs), station PFV is located in a favourable position with respect to the movement if the fault, while VJF is in an unfavourable position. Hence, the PGA at the 62.6km VJF station is comparable to that of the 40.3km PFV station, and some spectral components are higher in the VJF station (Figure 19). The same effect will be highlighted later as outcome of the modelling in Figure 29.

5. Design implications for stiff structures

One can notice that the high frequency content in the CAMUS study (Figure 6) is fairly low, compared to the values observed in the Kuovola earthquake, on bedrock. In order to emphasise further the effect of NF shaking to activating higher modes we compared the CAMUS building to the shaking measured in station KV03 component north. The CAMUS building has been a five story shear building, with constant stiffness distribution along the height, and equal floor masses (Figure 5). The concrete shear walls of the specimen were 1.7m long 0.06m thick and the total height 5.1m. The total mass was 36tonnes.

With a simple estimate of floor stiffness equal to 181kN/mm and floor masses of 7.2 tonnes for each floor we can estimate the five horizontal vibration frequencies to be $f_1=7.2\text{Hz}$, $f_2=21\text{Hz}$, $f_3=33\text{Hz}$, $f_4=42\text{Hz}$ and $f_5=48\text{Hz}$. Plotting these values over the KV03 spectra, filtered with high-pass over 0.25Hz, one can observe that the signal is significantly larger for modes 3, 4 and 5. It can also be noted that the input spectra is very small, with spectral ordinate of only 4mm/s^2 (0.0004g) at the first vibration frequency. All resulting forces and displacement will be very small, but the purpose of the calculation is to show the effect of the higher vibration modes.

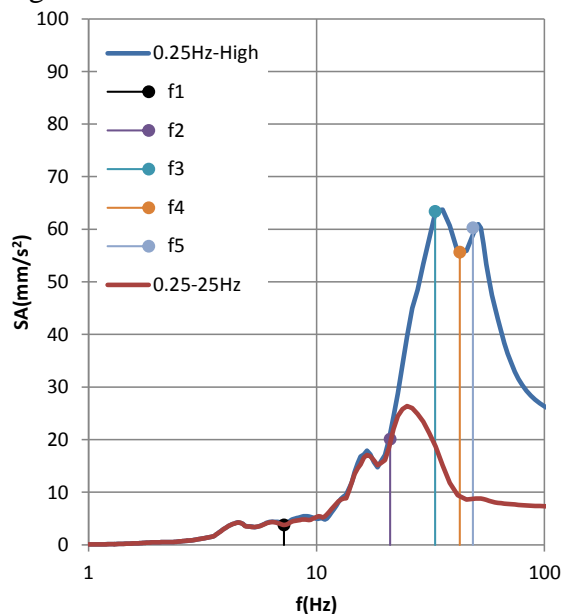


Figure 20. Estimated vibration frequencies of the CAMUS structure, overlapped on the pseudo-acceleration spectra of station KV03 component North

The structure was calculated using a 5DOF oscillator, directly carrying out time-history (TH) calculation to the KV03_bn signal with, and by decomposing the spectral contributions of each of the 5 modes and recombining them into the complete response. Since the structure has five dynamic degrees of freedom, once all modal contributions are summarised the results must equal that of the TH analysis. Damping was assumed 5% on all modes.

Three quantities were monitored – (1) the top displacement, (2) the bases-shear force and (3) the horizontal story shear of the 5th floor. The first two quantities are global measures of the response of the structure, while the third is a local measure.

In Figure 21 we present the base shear force estimates using the two analysis methods, time-history (TH) and modal decomposition of responses. As expected, the two calculations lead to

identical values. Further, in the Figure 22 we present the base-shear and top displacement of the structure as calculated from a TH analysis and as estimated only by using the response in the fundamental mode (7.2Hz). As it can be seen, the simplified estimate is giving a very reasonable value for both quantities.

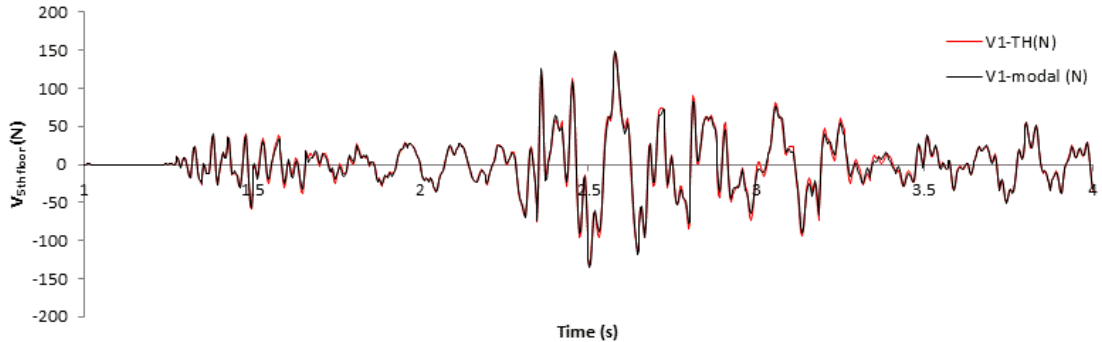
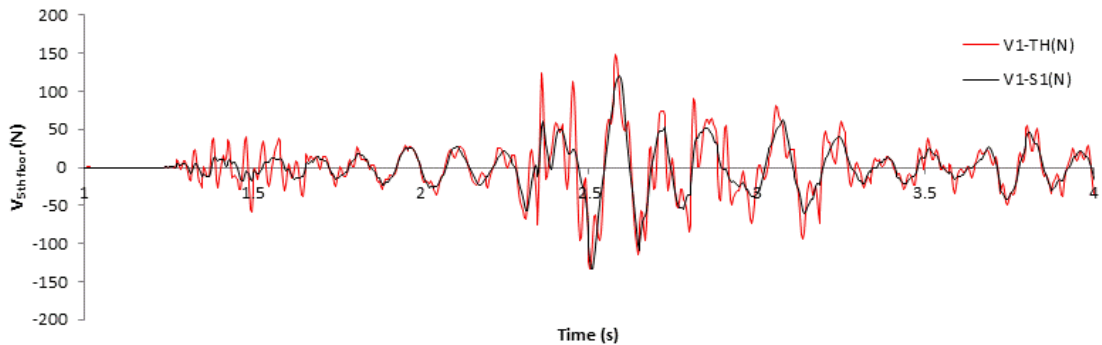
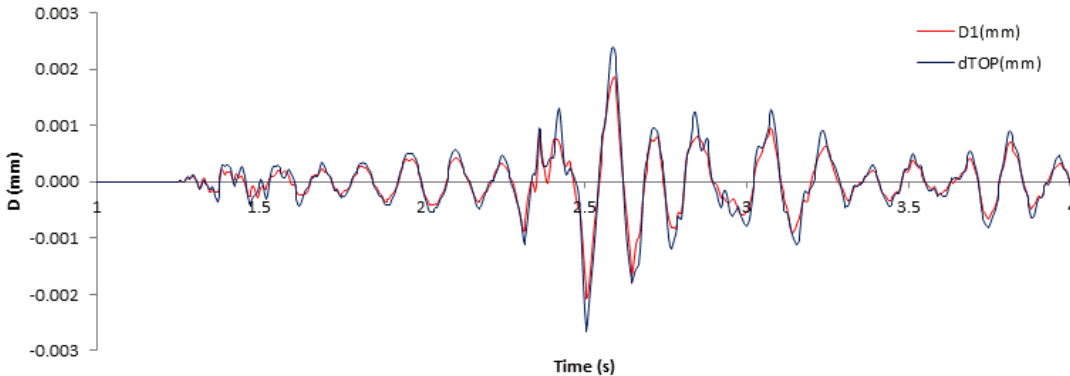


Figure 21. Base-shear force estimates from time-history (TH) analysis and re-composition of the five modal responses



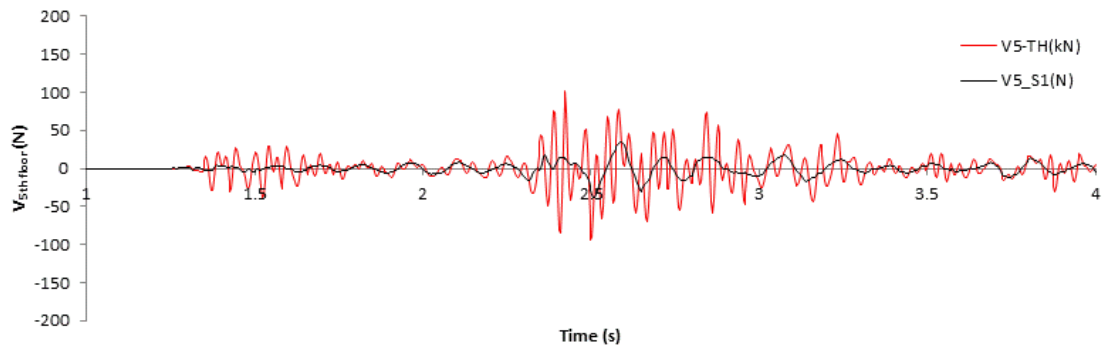
a)



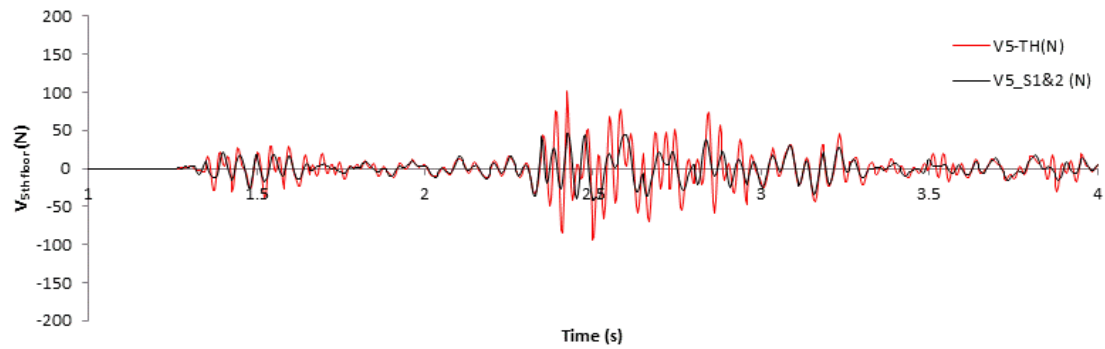
b)

Figure 22. (a) Base force from time-history (TH) analysis and 1st mode contribution and (b) top-floor displacement from TH analysis and 1st mode contribution.

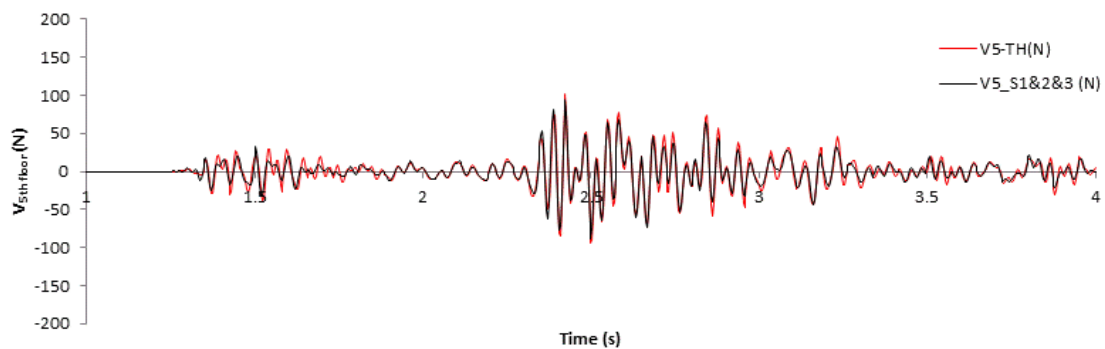
However, the situation is very different in Figure 23, where the 5th floor shear force is plotted. It can be observed that at least the first three modes are needed to reasonably estimate this quantity from a modal spectral simplified analysis (Figure 23.c). An estimate based on the 1st mode is completely inadequate (Figure 23.a), and the estimate based on the first two modes is also severely underestimating the 5th floor shear force (Figure 23.b).



a)



b)



c)

Figure 23. 5th floor shear force (a) from time-history (TH) analysis and 1st mode contribution only; (b) 1st and 2nd mode contribution and (c) 1st, 2nd and 3rd mode contributions.

It can be concluded that, in order to give a reasonable estimate for the 5th floor shear force in a modal-spectral calculation, one need to cover at least the first three vibrations modes. Since the third mode frequency is $f_3=33\text{Hz}$, the correct representation of the PSA spectra at least to that frequency is needed. A signal filtered to low upper cut-off frequency or a signal with inadequate sampling is not able to fulfil these conditions.

With larger magnitudes the fault size is larger and a different rupture time can be expected. Hence, the effect of magnitude increase on the tremor duration can be estimated. Beyond the fault itself, the larger the fault and magnitude the lower the frequency content will be, as more and more of the higher frequencies cancel out from interference during the rupture. If you are close to the fault, and the fault is long, then there is more uncertainty about the frequency content.

6. Rupture and ground motion modelling

A model was developed using the COMPSYN computer program to simulate rupture of faults and wave propagation to the Earth's surface (Spudich and Archuleta, 1987; Spudich and Xu, 2003). The modelling is compared to the Kouvola M_L 2.6 event, and primarily the measurements at the KV03 station. The work is ongoing and current status of the comparison work is reported here.

In COMPSYN, it is possible to model the fault, its rupture process and the propagation of waves up to an observer located on the ground surface. While there are several limitations discussed later, the program is very fast, one run taking only seconds to complete. An example of possible model arrangement is given in Figure 24.

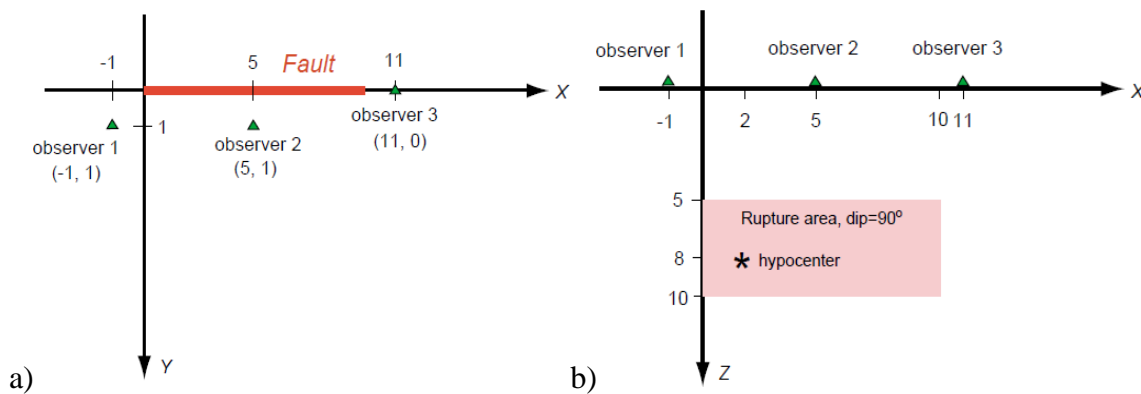


Figure 24. Top (a) and cross sectional (b) view of a vertical fault with rupture area of 10x5km. The hypocentre is marked and three observers are located on the ground surface (Spudich and Xu, 2003).

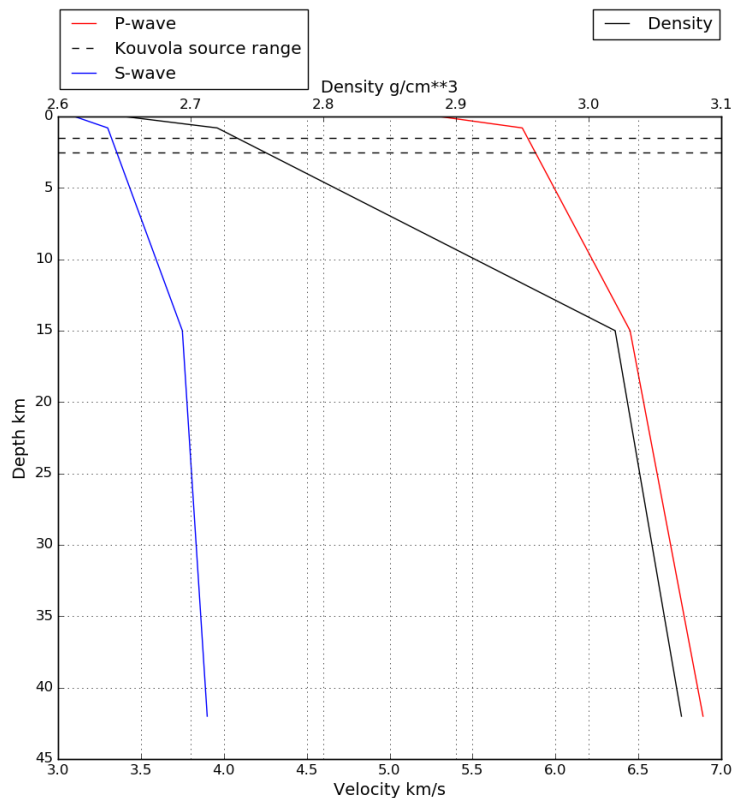


Figure 25. Crustal velocity model used in the COMSYN models

An important input parameter to the models is the crustal velocity model. Since only incomplete information usually exists of the local geology at depth, we reconstructed the velocity model presented in Figure 25 from different sources. The main input was the velocity model used by the Institute of Seismology at the University of Helsinki, correlated with data from Saari (1998), and near-surface properties adjusted with the borehole data from a nearby location at Loviisa NPP (Okko et al., 1999; Okko et al., 2000; Okko et al., 2003). The profile used in the models is presented in terms of pressure wave velocity (P-wave), shear-wave velocity (S-wave) and assumed density (Figure 25).

The generic representation of the fault in COMPSYN is given in Figure 26. The basic input to the model is the fault area and the slip. The slipping area in the models have been chosen to preserve compatibility with the estimated moment magnitude of the event, $M_w=2.3$. Hence, the slip area was estimated to be bounded between 100×100 m and 200×200 m (Leonard, 2010). This area was divided in 11×11 slipping patches. The rupture takes place in a circular area with radius of 100 and 200 meters, with the hypocentre located in the centre of the circular area.

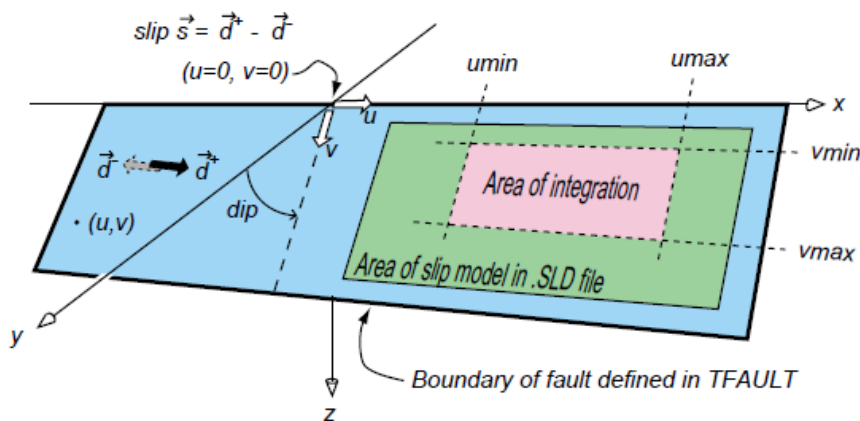


Figure 26. Generic representation of an earthquake fault in COMPSYN (Spudich and Xu, 2003). In the figure “x” is the strike direction, “dip” is the dip angle. “d” are the displacement vectors corresponding to movement of the fault; the slip “s” is calculated as the vector sum of displacements. The “u” and “v” values represent local coordinates of a point in the plane of the fault. Only a certain portion of the fault (defined in TFAULT) may be defined as slipping as given in the figure.

At this modelling stage we utilized the most basic form of slip-rate function presented in Figure 27.a, presuming a constant slip-rate or slip velocity during the entire time while a point on the fault slips (dashed lines). This assumption results in a linear increase of the slip with time (Figure 27.a – full line). The slip at each point on the fault is characterised by a rupture time, the time when the rupture arrives to that point (t_s) and a rise time, the time while the slip is continuing in that point (τ). If we assume the fault rupture propagating from the hypocentre towards the edges of the rupture area, it means that each point on the fault will start slipping at the moment when the rupture front from the hypocentre arrives to its position. A more complex representation of the fault slip is the modified Kostrov model, which was not yet employed in this study. However, the modified Kostrov model has been used to generate high-frequency synthetic seismograms.

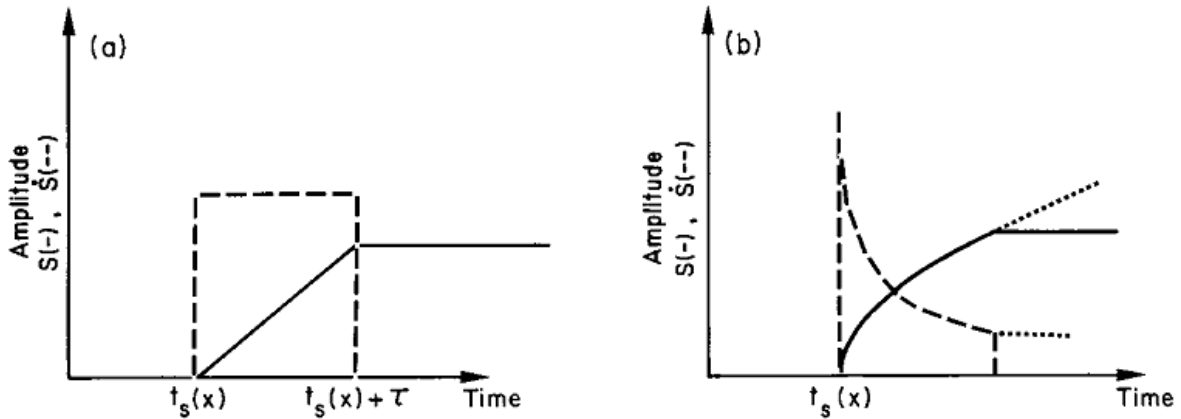


Figure 27. Possible slip and slip rate functions: (a) the Haskell model and (b) the modified Kostrov model (Spudich and Archuleta, 1987).

To define the time in all positions of the rupture area we assumed the following behaviour: (1) rupture starts at the centre of the circular rupture area (the hypocentre); (2) the rupture propagates toward the edges with a velocity of about $0.76 \times V_s$, the shear wave velocity; (3) once the rupture reached the edge there is a time lapse of 0.02s, and the “healing” starts to propagate from the edges towards the centre and (4) once the “healing” process reaches the hypocentre, the entire slip process stops. The time lapse was necessary in order to avoid very high slip rates on the edges of the rupture zone. If no time lapse is inserted, the “healing” is starting instantly, and the points very close to the edge slip rate approaches infinity. The healing velocity was assumed to exceed the rupture velocity and being the range of the shear wave velocity (Spudich and Archuleta, 1987). As a consequence, the rise time is longest in the hypocentre and it is equal to the time for the rupture propagating to the edges, plus the “healing” propagating from the edges to the hypocentre plus the 0.02s time lapse. On the other hand, the rise time of points close to the rupture edges is very small, on the edges equal to the time lapse only.

The slip displacement was assumed to parabolically decrease from the maximum value (D_{max}) at the centre of the fault towards the edge; with displacement at the edges being zero. This is an initial approximation, as slip may be concentrated on much smaller area even within an already small-size fault (Dreger et al., 2007), and alternative models exist for the estimation of D_{max} (Kim and Sanderson, 2005).

The mid-fault displacement was calibrated in order to achieve the desired moment magnitude:

$$M_w = \frac{2}{3} \cdot \log(M_0) - 6.03 \quad (1)$$

Where: M_w (=2.32) the moment magnitude as defined by Hanks and Kanamori (1979)
 M_0 is the seismic moment in [Nm]

M_0 is calculated is:

$$M_0 = \mu \cdot \sum A_i \cdot D_i \quad (2)$$

Where: M_0 is the seismic moment
 μ is the shear modulus of the rocks (Pa)

A_i is the area of the i^{th} individual slip patch (m^2)
 D is the assumed displacement of the i^{th} slip patch(m)

In the model all patch areas are equal and displacements are decreasing from the hypocentre to the edges. All patch areas displacements are summed for the entire slip area. The approximations of $\mu=32\text{GPa}$ has also been adopted.

Hence, the largest slip takes place at the centre patch of the circular fault, and there the slip time is long. On the other hand, for the points in the vicinity of the fault edge there is much smaller slip but also very little time. Hence, the slip velocity is increasing towards the edges of the fault. In fact, one reason for inserting the time-lapse is also to avoid extremely high slip-rates at the edges of the fault. The resulting rupture time and rise time are given in Figure 28.

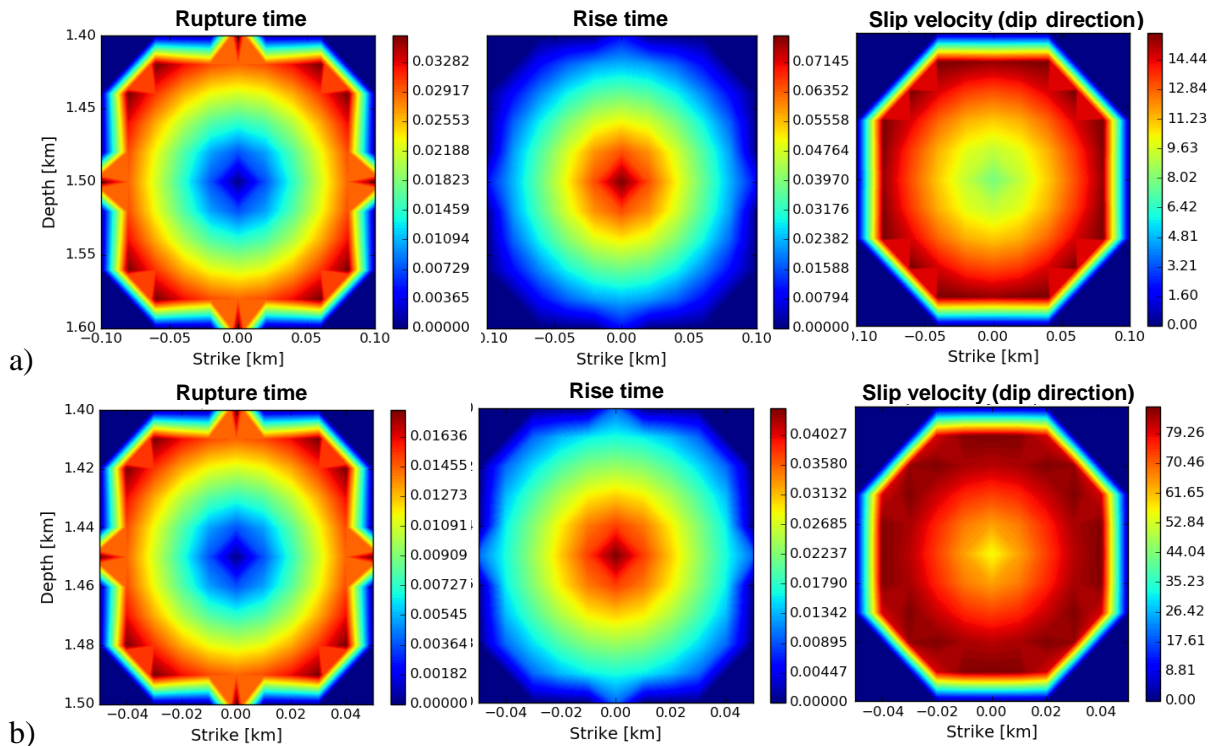
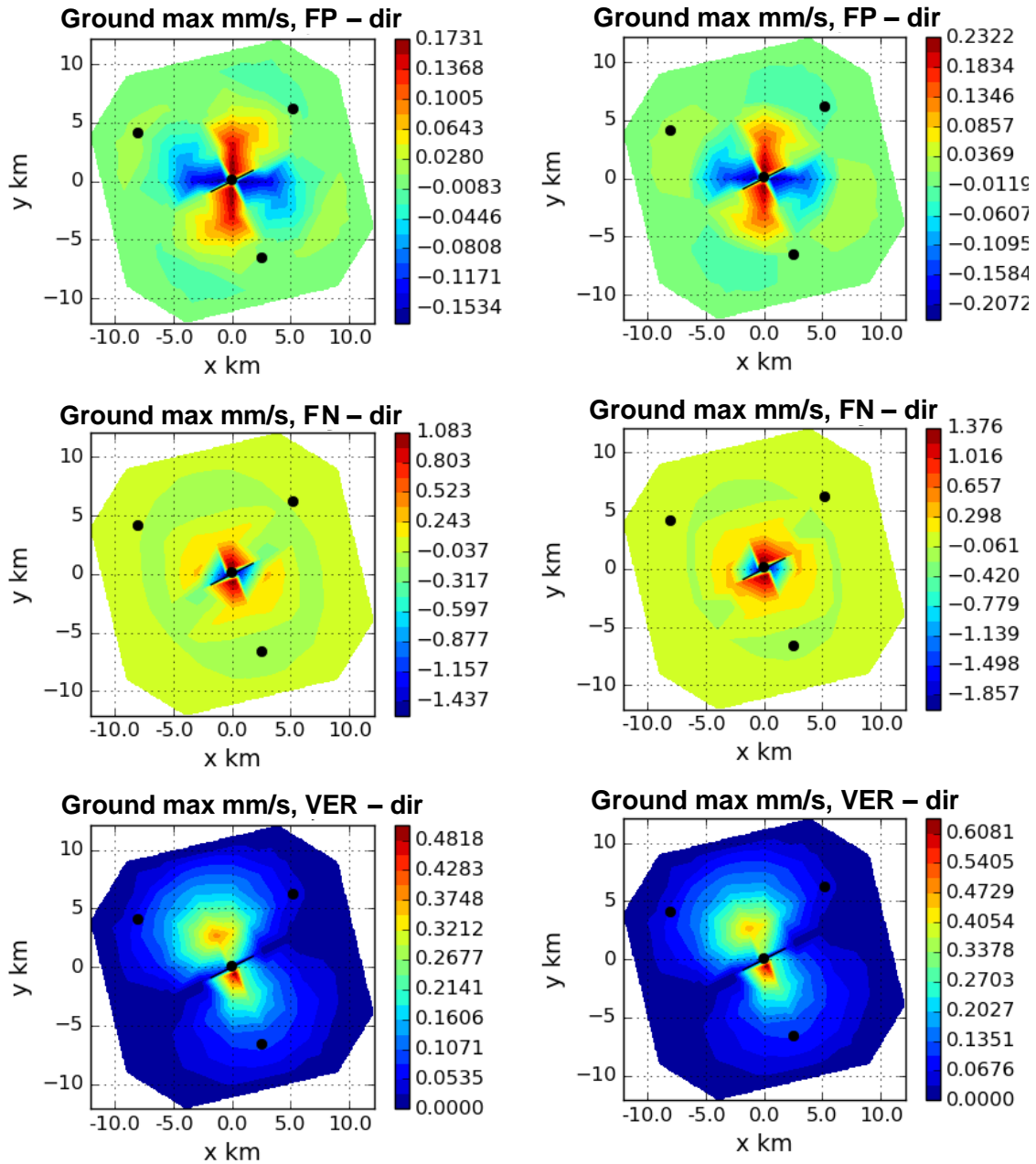


Figure 28. Rupture time and rise time in seconds (s) and slip velocity (cm/s) for the 200x200m (a) and the 100x100 (b) faults

The primary outputs of the models are plots of velocity on the ground surface resulting from the fault movement. Two example outputs are presented in Figure 29, for the model based on the fault plane solution given in Figure 13, with the simplification that only dip-direction movement was included. The velocities are measured in mm/s and are given for the direction parallel to the fault (FP) and the direction normal to the fault (FN), as well as vertical direction (VER). The plots were obtained by locating several observers (as in Figure 24) around the monitored area of about $20\times 20\text{km}$ and extracting the outputs with a self-developed PYTHON script.

The horizontal direction plots emphasize the pressure and tension quarters around the fault. The fault-normal (FN) components are an order of magnitude larger compared to fault-parallel (FP) components. This can be attributed to the movement of the fault which is dip-direction only. As strike-direction movement is added, the fault-parallel components of velocity

increases. The vertical direction velocity plot clearly emphasizes the movement of the fault in the dip-direction.



a) b)
Figure 29. Velocity plots for the model with the 200x200m (a) and the 100x100m (b) fault models. The black dots are the locations of the stations KV2, KV3 and KV4 (see also **Figure 18**). Fault is presented with a black line. Fault size is exaggerated in the pictures for clarity.

The KV stations are present in the plot as dark dots. At this stage of the study we are analysing the individual KV station outputs. Preliminary analysis shows that the models are able to capture the magnitude of velocities, at least in the in the KV3 station, where rock conditions are postulated.

7. Conclusions

This is the first progress year of the ADdGROUND project, so only preliminary conclusions can be presented. These are:

1. The recent PSHA studies, especially the de-aggregation results, suggest that the principal source of hazard to plants is within close range of the plant (~60km). In earthquake-engineering terms this range corresponds to epicentral, near-field and intermediate field sites. But the immediate vicinity of the plants (~5..20km) is usually well mapped for surface faults, and hence the potential of these sources is understood.
2. The scarcity of ground motion measurement data in this range is contributing to the uncertainties of the hazard studies, especially because GMPE's are calibrated with data from larger distances, where ground motion amplitudes are more homogeneous.
3. Ground motion amplitudes are always affected by the radiation pattern, creating ground motions with different amplitudes in the different propagation directions. However, in the close vicinity of the hypocentre, the nearness of the fault amplifies this effect and make it less straight forward to predict. Data emphasizing the amplitude differences is not available from measurements in Fennoscandia, because of the small events and small size of the faults.
4. From measurements with high sampling of very small events ($M_L 2.6$, $M_w 2.3$), some near-source effects can be confirmed – these are: shorter duration (Figure 12, KV stations), the presence of very high frequency components in the shaking (Figure 17, especially KV03) and relatively high value of the vertical shaking component (Figure 17, KV03). Some of the stations were, unfortunately, not located on bedrock making interpretation difficult.
5. Other near source effects, like fault directivity would be easier to observe on events with the range of magnitudes within the design range e.g. $M=5$.
6. Near-source effects are not of the nature to endanger the structures of a nuclear plant designed to a comparable magnitude far-field earthquake; however they need to be considered for qualification of equipment.
7. Modelling of the source has the potential to predict some features of the near-source ground motions. This allows for studying the effects of different focal mechanisms, and to extrapolate results to larger events, where measurements are lacking.
8. So far, we improved our modelling capability in COMPSYM, developed interpretation tools for result extraction and made a preliminary calibration of models to a small local earthquake in Kouvola, Finland.

Plans for 2016 within the project:

1. With the tools developed in 2015 we intend to further improve the model calibration based on the Kouvola event.
2. Extend the study to higher shaking frequencies. So far, we managed to compare model output with measurements up to about 3-4Hz.
3. Extend the study to $M5-5.5$ earthquakes, more within the interest range of safety studies for nuclear plants.

8. Acknowledgment

NKS conveys its gratitude to all organizations and persons who by means of financial support or contributions in kind have made the work presented in this report possible.

9. Disclaimer

The views expressed in this document remain the responsibility of the author(s) and do not necessarily reflect those of NKS. In particular, neither NKS nor any other organisation or body supporting NKS activities can be held responsible for the material presented in this report.

10. References

- ASCE, 2005. Seismic Design Criteria for Structures, Systems, and Components in Nuclear Facilities. American Society of Civil Engineers, Reston, Virginia.
- Brune, J.N., 1970. Tectonic stress and the spectra of seismic shear waves from earthquakes. *J. Geophys. Res.* 75, 4997–5009. doi:10.1029/JB075i026p04997
- Connor, C.B., Chapman, N.A., Connor, L.J., 2009. Volcanic and Tectonic Hazard Assessment for Nuclear Facilities. Cambridge University Press.
- Constantopoulos, I.V., Ries, E.R., Michalopoulos, A.P., 1980. Progress Report - Recent Experience from the Practice of Seismic Analysis for Structures, in: Proceedings of the 7th World Conferences on Earthquake Engineering. Presented at the 7th World Conferences on Earthquake Engineering, Istanbul, Turkey, pp. 197–212.
- Dreger, D., Nadeau, R.M., Chung, A., 2007. Repeating earthquake finite source models: Strong asperities revealed on the San Andreas Fault. *Geophys. Res. Lett.* 34, L23302. doi:10.1029/2007GL031353
- Follow-up IAEA Mission in Relation to the Findings and Lessons Learned from the 16 July 2007 Earthquake at Kashiwazaki-Kariwa NPP - Volume I (Mission Report), 2008. . International Atomic Energy Agency (IAEA), yo and Kashiwazaki-Kariwa NPP, Japan.
- Fülöp, L., Jussila, V., Malm, M., Tiira, T., Saari, J., Li, Y., Mäntyniemi, P., Heikkinen, P., Puttonen, J., 2015. Seismic Safety of Nuclear Power Plants - Targets for Research and Education (SESA) - Final Report, in: SAFIR2014, The Finnish Research Programme on Nuclear Power Plant Safety 2011-2014, (Final Report), VTT Technology. VTT Technical Research Centre of Finland, Espoo, pp. 604–619.
- Gioncu, V., Mazzolani, F.M., 2011. Earthquake engineering for structural design. Spon Press, London ; New York.
- Gioncu, V., Mosoarca, M., Anastasiadis, A., 2014. Local ductility of steel elements under near-field earthquake loading. *J. Constr. Steel Res.* 101, 33–52. doi:10.1016/j.jcsr.2014.05.001
- GTK, 2015. Superficial deposits maps (Maankamara).
- Hall, J.F., Heaton, T.H., Halling, M.W., Wald, D.J., 1995. Near-Source Ground Motion and its Effects on Flexible Buildings. *Earthq. Spectra* 11, 569–605. doi:10.1193/1.1585828
- Hanks, T., Kanamori, H., 1979. A Moment Magnitude Scale. *J. Geophysical Res.* 84.
- Havskov, J., Ottemoller, L., 1999. SeisAn Earthquake analysis software. *Seis Res Lett* 70.
- Huang, C., 2003. Considerations of Multimode Structural Response for Near-Field Earthquakes. *J. Eng. Mech.* 129, 458–467. doi:10.1061/(ASCE)0733-9399(2003)129:4(458)
- IAEA, 2002. Evaluation of Seismic Hazards for Nuclear Power Plants, Safety Guide - NS-G-3.3.
- Internet Site for European Strong-Motion Data [WWW Document], n.d. URL http://www.isesd.hi.is/ESD_Local/frameset.htm (accessed 2.4.16).
- Kalkan, E., Reyes, J.C., 2013. Significance of Rotating Ground Motions on Behavior of Symmetric- and Asymmetric-Plan Structures: Part II. Multi-Story Structures. *Earthq. Spectra* 31, 1613–1628. doi:10.1193/072012EQS242M
- Kim, Y.-S., Sanderson, D.J., 2005. The relationship between displacement and length of faults: a review. *Earth-Sci. Rev.* 68, 317–334. doi:10.1016/j.earscirev.2004.06.003
- Korja, A., Kosonen, E., 2015. Seisotronic Framework and Seismic Source Area in Fenniscandia, Northern Europe (No. REPORT S - 63). Institute of Seismology, University of Helsinki, Helsinki, Finland.

- Kostov, M., 2001. Seismic Re-evaluation of Kolzoduy NPP Criteria, Methodology, Implementation, in: Workshop on the Seismic Re-Evaluation of All Nuclear Facilities. Presented at the Workshop on the Seismic Re-evaluation of all Nuclear Facilities, Organisation for Economic Co-operation and Development (OECD, Ispra, Italy).
- Labbé, P., 2001. Seismic Re-evaluation of Existing Nuclear Power Plants An Introduction to an IAEA Safety Report, in: Workshop on the Seismic Re-Evaluation of All Nuclear Facilities. Presented at the Workshop on the Seismic Re-evaluation of all Nuclear Facilities, Organisation for Economic Co-operation and Development (OECD, Ispra, Italy).
- Labbé, P., Altinyollar, A., 2011. Conclusions of an IAEA–JRC research project on the safety significance of near-field seismic motions. Nucl. Eng. Des., ICONE-17: Heavy Liquid Metal Technologies and Material Challenges for Gen IV Fast Reactors 241, 1842–1856. doi:10.1016/j.nucengdes.2011.02.006
- Leonard, M., 2010. Earthquake Fault Scaling: Self-Consistent Relating of Rupture Length, Width, Average Displacement, and Moment Release. Bull. Seismol. Soc. Am. 100, 1971–1988. doi:10.1785/0120090189
- Malm, M., Saari, J., 2014. SESA, Subproject 1 - Earthquake Hazard Assessment, Progress Report 2014 (Research Report No. DSAF14R). ÅF-Consult Ltd.
- McGuire, R.K., 1976. FORTRAN Computer Program for Seismic Risk Analysis (No. 76-67). US Department of the Interior / US Geological Survey.
- NRA, 2013. 基準地震動及び耐震設計方針に係る審査ガイド (Examination guide according to the reference ground motion and seismic design policy).
- Okko, O., Front, K., Anttila, P., 2003. Low-angle fracture zones in rapakivi granite at Hästholmen, southern Finland. Eng. Geol. 69, 171–191. doi:10.1016/S0013-7952(02)00281-8
- Okko, O., Front, K., Hassinen, P., 1999. Loviisan Hästholmenin kairanreikien KR7 ja KR8 geofysikaalisten reikämittausten tulokäsittely sekä kallioperän rakennemallin tarkastelu (No. Workreport 1999-48). Posiva Oy.
- Okko, O., Front, K., Hassinen, P., Paulamäki, S., Paananen, M., 2000. Loviisan Hästholmenin kairanreiän KR9 geofysikaalisten mittausten tulokäsittely ja kallioperämallien tarkastelu (No. Workreport 2000-24). Posiva Oy.
- Ottmøller, L., Voss, P., Havskov, J., 2014. SEISAN earthquake analysis software for Windows, Solaris, Linux and MacOS. Department of Earth Science, Norway & Geological Survey of Denmark and Greenland, 2014.
- Preliminary findings and lessons learned from the 16 July 2007 earthquake at Kashiwazaki Kariwa NPP - The Niigataken Chuetsu-Okai Earthquake (Volume I) (Mission Report), 2007. . International Atomic Energy Agency (IAEA), Kashiwazaki-Kariwa NPP and Tokyo, Japan.
- Reyes, J.C., Kalkan, E., 2015. Significance of Rotating Ground Motions on Behavior of Symmetric- and Asymmetric-Plan Structures: Part I. Single-Story Structures. Earthq. Spectra 31. doi:10.1193/072012EQS241M
- Saari, J., 1998. Regional and local seismotectonic characteristics of the area surrounding the Loviisa nuclear power plant in SE Finland (PhD Thesis, Report S-36). Institute of Seismology, University of Helsinki, Helsinki, Finland.
- Smedberg, I., Uski, M., Tiira, T., Komminaho, K., Korja, A., 2012. Intraplate earthquake swarm in Kouvola, south-eastern Finland, in: EGU General Assembly Conference Abstracts. Presented at the EGU General Assembly Conference Abstracts, p. 8446.

- Smedberg, I., Uski, M., Tiira, T., Korja, A., Komminaho, K., 2012. Shallow swarm-type earthquakes in south-eastern Finland, in: The 43rd Nordic Seismology Seminar. Presented at the The 43rd Nordic Seismology Seminar, Tallinn.
- Spudich, P., Archuleta, R.J., 1987. Techniques for Earthquake Ground-Motion Calculation with Applications to Source Parameterization of Finite Faults, in: Seismic Strong Motion Synthetics. Elsevier, pp. 205–265.
- Spudich, P., Xu, L., 2003. 85.14 Software for calculating earthquake ground motions from finite faults in vertically varying media, in: William H.K. Lee, H.K., Paul C. Jennings and Carl Kisslinger (Ed.), International Geophysics, International Handbook of Earthquake and Engineering Seismology. Academic Press, pp. 1633–1634.
- Stevenson, J.D., 2014. Summary of the historical development of seismic design of nuclear power plants in Japan and the U.S. Nucl. Eng. Des., Special Issue - The International Conference on Structural Mechanics in Reactor Technology (SMiRT21), New Delhi India, Nov 06-11, 2011 269, 160–164. doi:10.1016/j.nucengdes.2013.08.023
- Vuorinen, T., 2015. New Fennoscandian Ground Motion Characterization Models (MSc thesis). University of Helsinki, Helsinki, Finland.
- YVL 2.6, 2001. Seismic events and nuclear power plants, Finnish Regulatory Guide on Nuclear Safety (YVL).
- YVL B.7, 2013. Provisions for internal and external hazards at a nuclear facility, Finnish Regulatory Guide on Nuclear Safety (YVL).

Appendix A: Program of the workshops organized in 2015 in the ADdGROUND project



The Technical Research Center of Finland cordially invites you to the workshop on

Potential of numerical methods to supplement empirical earthquake observations

When: 8th May 2015, 10.00-13.00
Where: Room Aari, Tekniikantie 1, Espoo

Background

Significant hazard to a site in Fennoscandia is generated from mid-magnitude seismic event with epicenter localized in the proximity. Earthquake source modeling can be used to understand vibrations in areas close to the earthquake epicenters; but source modeling in stable continental region has limited research background. Different modeling techniques were used for modeling fault stresses/rupture in glaciation scenarios (Lund & Schmidt, 2011) and earthquakes Fälth *et al* (2014).

Uncertainty in such complex models is significant. Measured data from earthquakes and/or explosions can be used to calibrate models. This type of data being rare, the goal of the Workshop is to identify and share relevant Nordic data for the purpose.

References:

- B. Lund, P. Schmidt, *Stress Evolution and Fault Stability at Olkiluoto During the Weichselian Glaciation*, Working Report 2011-14
- Fälth, B., H. Hökmark, B. Lund, P.M. Mai, R. Roberts, R. Munier (2015) Simulating earthquake rupture and off-fault fracture response: Application to the safety assessment of the Swedish nuclear waste repository, *Bull. Seismol. Soc. Am.*, 105, 134-151, doi: 10.1785/0120140090

Workshop program

10.00 – 11.00

- Earthquake hazard estimations for southern Scandinavia (Peter H. Voss)
- Recent developments of the Fennoscandian shield ground motion characterization models (Tommi Vuorinen, Timo Tiira, Björn Lund, Marja Uski)
- Simulation of earthquake rupture using 3DEC (Billy Fälth)

Coffee break

11.20 – 12.20

- Overview of the M4.1 Sveg earthquake of Sep 15, 2014 (Björn Lund)
- Seismic recordings of Posiva (Jouni Saari)
- Characterization of the Kouvola data from 2012 (Vilho Jussila, Ludovic Fülöp)

12.30-13.00 Discussion and conclusions

Welcome!

Organizer:



Project partners:



UPPSALA
UNIVERSITET



UNIVERSITY OF HELSINKI



Supported by:



Nordic nuclear safety research

The workshop is organized within the project "Modelling as a tool to augment ground motion data in regions of diffuse seismicity" (ADdGROUND / NKS_R_2015_113).

Local organizer
Name: Ludovic Fülöp
Mob. +358 40 593 4698
E-mail: ludovic.fulop@vtt.fi

The
Geological Survey of Denmark and Greenland
and the
Technical Research Center of Finland
cordially invites you to the workshop on

Potential of numerical methods to supplement empirical earthquake observations

When: 15th Dec 2015, 10.00-13.00
Where: Øster Voldgade 10, Copenhagen

Background

Significant hazard to a site in Fennoscandia is generated from mid-magnitude seismic event with epicenter localized in the proximity. Earthquake source modeling can be used to understand vibrations in areas close to the earthquake epicenters; but source modeling in stable continental region has limited research background. Different modeling techniques were used for modeling fault stresses/rupture in glaciation scenarios (Lund & Schmidt, 2011) and earthquakes Fälth *et al* (2014).

Uncertainty in such complex models is significant. Measured data from earthquakes can be used to calibrate models. The goal of the workshop is to discuss modeling techniques and present exploratory modelling work.

References:

- B. Lund, P. Schmidt, *Stress Evolution and Fault Stability at Olkiluoto During the Weichselian Glaciation*, Working Report 2011-14
- Fälth, B., H. Hökmark, B. Lund, P.M. Mai, R. Roberts, R. Munier (2015) Simulating earthquake rupture and off-fault fracture response: Application to the safety assessment of the Swedish nuclear waste repository, *Bull. Seismol. Soc. Am.*, 105, 134-151, doi: 10.1785/0120140090

Workshop program

10.00 – 11.00

- Seismic studies with safety focus to NPP's (Ludovic Fülöp)
- Swam events in Finland (Peter H. Voss)
- Parameters and exploratory models for the ML2.6 Kouvola earthquake (Vilho Jussila, Ludovic Fülöp, Björn Lund, Billy Fälth)

Coffee break

11.20 – 12.20

- Implementation and tests of spontaneous rupture models (Billy Fälth)
- Preliminary calibration results from the Baltic Sea 1.7 ton blast on 18 November 2015 (Björn Lund)

12.30-13.00 Discussion and conclusions

Welcome!

The workshop is organized within the project "Modelling as a tool to augment ground motion data in regions of diffuse seismicity" (ADdGROUND / NKS_R_2015_113).

Local organizer

Name: Peter Voss
Phone: +45 40 21 62 88
E-mail: pv@geus.dk

Organizer:



GEUS

Project partners:



UPPSALA
UNIVERSITET



UNIVERSITY OF HELSINKI



Aalto-yliopisto



Supported by:

nks

Nordic nuclear safety research

Title	Modelling as a tool to augment ground motion data in regions of diffuse seismicity - Progress 2015
Author(s)	Ludovic Fülöp ¹ , Vilho Jussila ¹ , Björn Lund ² , Billy Fälth ² , Peter Voss ³ , Jari Puttonen ⁴ , Jouni Saari ⁵ , Pekka Heikkinen ⁶
Affiliation(s)	¹ VTT Technical research Centre in Finland Oy, ² Uppsala University, ³ Geological Survey of Denmark and Greenland, ⁴ Aalto University, ⁵ ÅF Consult Oy, ⁶ Institute of Seismology, University of Helsinki
ISBN	978-87-7893-448-2
Date	May 2016
Project	
No. of pages	38
No. of tables	0
No. of illustrations	29
No. of references	39
Abstract max. 2000 characters	<p>De-aggregation of probabilistic hazard assessment (PSHA) results show that the dominating source of vibrations with engineering significance to NPP safety is from mid-magnitude earthquakes located at close distances to the plant. This region is called the “near-field” and is known for its particularities when compared to “far-field”. For example, significant duration of the ground motions is shorter, corresponding to S-wave and surface wave arrivals; there are distinctive high velocity peaks in the ground motions and vertical shaking components may exceed horizontal components. These particularities are known to have design consequences, but are often overlooked by engineering codes.</p> <p>In Fennoscandia, near-field observations of larger magnitude ($M > 3$) earthquakes are missing, and modelling is the only way to supplement the existing empirical data underpinning the attenuation equations in the PSHA studies.</p> <p>In the ADdGROUND project, during the financial year 2015, we confirmed the near-source effect in small magnitude earthquake recordings in Finland and developed modeling skills and tools to generate synthetic near-field accelerograms starting from process of the fault rupture. We calibrated models with the very few existing</p>

near-field measurement cases of small earthquakes. In this report we also highlight some of the potential design consequences of near-source earthquakes to nuclear installations. The consensus seems to be that the destructive potential of these types of earthquakes is generally low. However, they can produce surprisingly larger acceleration values in the range of high frequencies, and can generate high strain rates in the loaded structures and components. In nuclear installations, with stiff components the effect of high frequency shaking should be carefully considered.

Within the ADdGROUND activity we organized two workshops, one on the 8th May 2015 in Espoo, and the second in Copenhagen (15th December 2015). The outcomes have been presented to the nuclear community in the Nordic countries in the NKS Seminar “Nordic perspectives of Fukushima: Where are we now and where do we go? Joint NKS-R and NKS-B Seminar” in Stockholm (12-13.01.2016).

Key words

nuclear power plant safety, earthquake, near-field effects, fault source modeling